Palynology and weathering proxies reveal climatic fluctuations during the Carnian Pluvial Episode (CPE) (late Triassic) from marine successions in the Transdanubian Range (western Hungary)

Viktória Baranyi, Ágnes Rostási, Béla Raucsik, Wolfram Michael Kürschner

PII: S0921-8181(18)30489-2
DOI: https://doi.org/10.1016/j.gloplacha.2019.01.018
Reference: GLOBAL 2905

To appear in: *Global and Planetary Change*

Received date: 11 September 2018
Revised date: 16 January 2019
Accepted date: 28 January 2019

Please cite this article as: V. Baranyi, Á. Rostási, B. Raucsik, et al., Palynology and weathering proxies reveal climatic fluctuations during the Carnian Pluvial Episode (CPE) (late Triassic) from marine successions in the Transdanubian Range (western Hungary), Global and Planetary Change, https://doi.org/10.1016/j.gloplacha.2019.01.018

Palynology and weathering proxies reveal climatic fluctuations during the Carnian Pluvial Episode (CPE) (Late Triassic) from marine successions in the Transdanubian Range (western Hungary)

Viktória Baranyi[a*], Ágnes Rostási[b], Béla Raucsik[c], Wolfram Michael Kürschner[a]

[a]Department of Geosciences, University of Oslo, P.O. Box 1047, Blindern, 0316 Oslo, Norway

[b]Department of Earth and Environmental Sciences, University of Pannonia, P.O.Box 158, H-8201 Veszprém, Hungary

[c]Department of Mineralogy, Geochmistry, and Geochemistry, University of Szeged, Egyetem utca 2–6, H-6722 Szeged, Hungary

*Corresponding author.

E-mail address: wycky87@gmail.com

Abstract

In the early Late Triassic, the Carnian Pluvial Episode (CPE) is a phase with increased siliciclastic influx into the marine-carbonate dominated depositional setting of the Western Tethys assumingly caused by a shift to more humid climatic conditions and increased continental runoff. Here, vegetation changes inferred from the palynological assemblages and weathering proxies (α^{Al}_{i}) have been studied from the Transdanubian Range (TR), western Hungary to reveal climate variations and detect episodes with hygrophytic vegetation and enhanced continental hydrolysis. Palynostratigraphy has been applied to correlate the clastic pulses known from elsewhere in the Western Tethys. The quantitative palynological analysis indicates a shift towards hygrophytic elements in the Julian 2, and return to xerophytic associations in the Tuvalian. The increase in the hygrophytic vegetation elements is coincident with elevated kaolinite and partially with the increase of α-values indicating strong terrestrial runoff, enhanced continental hydrolysis and more humid climate in the lower part of the Veszprém Formation in the early Julian 2. The wetter conditions in the Julian 2 were periodically interrupted by shorter periods of drier climate manifested in the progradation of carbonate platforms and the deposition of carbonate series and breccias interbedded between the marl units. In the late Julian 2 the high amount of hygrophytes points to another humid episode, but the decrease of kaolinite in the clay mineral profile and the weathering indices might suggest stronger seasonality. Although, the multiple clastic pulses in the western Tethys were related primarily to more humid climate during the CPE, the comparison to clay mineralogy and weathering proxies suggest a more complicated scenario in the TR. The enhanced continental weathering related to a more humid climate is only suggested for the lower part of the Veszprém Formation in the early stages of the CPE in the Julian 2.

1. Introduction

During the so called Carnian Pluvial Episode (CPE), the Western Tethys areas experienced a significant change in depositional style and an increase in the terrestrial influx within the marine sedimentary basins (e.g., Schlager & Schöllnberger, 1974; Hornung & Brandner 2005; Haas et al. 2012; Ogg 2015; Ruffell et al. 2016). This environmental change is assumed to be linked to a geologically short-lived episode with relatively higher precipitation (Roghi et al. 2010; Dal Corso et al. 2015, 2018) within the Late Triassic which was otherwise characterized by predominantly arid climate in low-mid latitudes with strong seasonality and a monsoonal regime (Kutzbach & Gallimore 1989; Parrish 1993; Sellwood & Valdes 2006). However, the climatic interpretation of the CPE is still widely debated (e.g., Dal Corso et al. 2019). Palaeoclimate proxies (e.g., low maturity Carnian sandstones, clay mineral profiles and paleosols indicative of high evaporation rates) do not point to a consistent climate change across European successions (e.g., Franz et al. 2018). Some works suggest only minor climate change with a generally arid to semi-arid background climate (from the UK Baranyi et al. 2018; from Spain Barrenechea et al. 2018), while data from the Germanic Basin argue for a uniform arid to semi-arid Carnian climate (Visscher et al. 1994). Lindström et al. (2017) did not record any humidity signal from the mid- to late Carnian series of the Danish Basin, which may suggest that the area was probably arid even during the CPE indicated by a palynologically barren interval in the Carnian. The interpretation of the CPE in the Western Tethys suggests the alternation of wet-dry episodes and distinct humid pulses during the late Julian and early Tuvalian (Breda et al. 2009; Roghi et al. 2010), before the climate returned to persistent aridity in the late Carnian and Norian (e.g., Preto et al. 2010). The question arises whether the discrepancy in the recorded climatic and environmental signal across the CPE is related to the contrast in the climate of the different regions. Eventually stratigraphic gaps in some continental series of Germanic Realm might be also related to the lack of the CPE signal.

The CPE is accompanied by sea level changes (e.g., Franz et al. 2014), global warming (e.g., Trotter et al. 2015; Sun et al. 2016; Hornung et al. 2007a, b, Rigo & Joachimski 2010), increased continental weathering (Rostási et al. 2011), demise of carbonate platforms (e.g., Keim et al. 2006; Hornung et al. 2007b; Breda al. 2009; Lukeneder et al. 2012), deepening of the CCD (Rigo et al. 2007) and locally oxygen depletion in marginal marine settings (e.g., Keim et al. 2006; Hornung et al. 2007b). Multiple negative carbon isotope excursions (NCIE) both in the marine and terrestrial realms (e.g., Dal Corso et al. 2012, 2015; Sun et al. 2016; Miller et al. 2017; Dal Corso et al. 2018) suggest the injection of a significant amount of ^{13}C-depleted CO_2 into the ocean-atmosphere-soil system during the CPE (Dal Corso et al. 2015, 2018). Currently four NCIEs are recognized in the western Tethys: at the Julian 1/2 boundary, in the Julian 2, at the Julian/Tuvalian boundary and at the base of the Tuvalian 2 (Dal Corso et al. 2018). Volcanism and associated feedbacks (methane clathrate dissolution, warming, and reduction in marine primary productivity) are the most likely triggers for the injection of ^{13}C-depleted CO_2. The emplacement of the Wrangellia Large Igneous Province could have been one of the main volcanic sources (e.g., Furin et al. 2006; Dal Corso et al. 2012, 2015, 2018).

The CPE environmental perturbations are closely associated with biotic turnovers among marine and terrestrial groups e.g., extinction of the *Trachyceratinae* ammonoids (e.g., Balini et al. 2010), conodont and crinoid extinction (Simms et al. 1995; Rigo et al. 2007; Chen et al. 2015; Dal Corso et al. 2018). Proceeding the CPE the environmental changes led to the extinction of several tetrapod groups and the first major diversification of the dinosaurs (Benton et al. 2018; Bernardi et al. 2018).

Palaeobotany and palynology have been widely applied in reconstructing climatic fluctuations during the CPE (e.g., Roghi et al. 2010; Mueller et al. 2016a, b; Baranyi et al. 2018). In the terrestrial floras and palynological records, an increase in the hygrophytic floral elements characterize the CPE which has been linked to a presumably more humid climate (Roghi 2004;

Roghi et al. 2010; Mueller et al. 2016a, b). In order to trace climatic variations, the palynological assemblages are studied from three borehole sections from the Transdanubian Range (TR) of western Hungary. The TR was part of the Western Tethys margin during the Late Triassic (Haas & Budai 1995). The large amount of siliciclastic input resulted in a drastic change in the depositional style of the Carnian marine successions and a switch from pelagic and platform carbonates to marls (Budai et al. 1999; Haas et al. 2012). The palynological analysis here is integrated with elemental values used as geochemical weathering proxies (α^{Al}_{i} of Garzanti et al. 2013) and the existing clay mineral record of Rostási (2011) and Rostási et al. (2011). The vegetation data inferred from palynology combined with clay mineralogy and the calculated chemical indices of weathering can be powerful tools for the interpretation of palaeoclimate (Ruffell et al. 2002; Dera et al. 2009; Raucsik & Varga 2008; Rostási et al. 2011; Haas et al. 2012) when used in conjunction (Sladen & Batten 1984; Ruffell et al. 2002). They can confirm episodes with the development of hygrophytic vegetation and enhanced continental weathering in the hinterland.

2. Geological setting

The Transdanubian Range (TR) located in the NW part of the Carpathian-Pannonian Basin (Fig. 1) is the northwestern segment of the ALCAPA terrane (Alpine-West Carpathian-Pannonian) (Fig. 1). During the Late Triassic the TR formed a segment of the passive Western Tethys margin and was situated between the Northern Calcareous Alps and the Southern Alps (Haas et al. 1995) (Fig. 1). The ALCAPA terrane reached its present-day position due to its eastward escape from the Alpine sector in the Paleogene-early Miocene (mainly Oligocene) (e.g., Kázmér & Kovács 1985; Csontos et al. 1992; Fodor et al. 1999) and a significant counter-clockwise rotation (e.g., Márton & Fodor 2003). The TR is made up predominantly of Triassic formations with a total thickness of 3–4 km (Figs 1-2). The Late Permian-Early

Triassic facies evolution is characterized by marine transgression and the flooding of the evaporitic alluvial plains and coastal lagoons leading to the formation of a shallow mixed siliciclastic-carbonate ramp (e.g., Haas & Kovács 2012; Haas et al. 2012). In the Middle Triassic, the extensional tectonic movements in the western end of the eastward progressing Neotethys resulted in the differentiation of the shelf and the former carbonate ramp in the TR became dissected (e.g., Budai et al. 1999; Budai & Vörös 2006; Haas & Kovács 2012). The depositional environment with the hemipelagic basins, deep troughs divided by isolated platforms was dominated by the sedimentation of pelagic and platform carbonates until the early Carnian (e.g., Budai & Vörös 2006). The Carnian sedimentary succession records the infilling of these hemipelagic basins due to the drastic increase in the siliciclastic input from the Julian 2 represented by the up to 800 m thick, mixed carbonate–siliciclastic sedimentary succession of the Veszprém Formation (e.g., Haas et al. 2012) (Figs 1-2). However, in some places evolution of carbonate platforms continued, e.g., in the area of the Keszthely Mountains (Ederics Formation) and in the eastern part of the Bakony (Sédvölgy Dolomite) (Figs 1-2). The gradual infilling of the hemiplegic basins led to a general transition from pelagic to shallow-water palaeoenvironments ended by the late Tuvalian, establishing the extremely levelled topography for the deposition of the Main Dolomite and Dachstein Limestone.

2.1. Veszprém Formation in the Balaton Highland and Bakony Mountains area

In the Balaton Highland-Bakony Mountains area two borehole sections were studied: Mencshely-1 (Met-1) and Veszprém-1 (V-1) (Fig. 1) The Met–1 represents a basin profile, while the V–1 is a slope succession, transitional between the pelagic basins and the carbonate platforms (Haas & Budai 1999). In the Balaton Highland-Bakony Mts., the Veszprém Formation develops (VMF) from the underlying pelagic limestone sequences of the Füred Formation (Figs 2-3), which composed of micritic limestone layers with thin marl

intercalations in its uppermost (early Julian) part. The Veszprém Formation is divided into four members: Mencshely Marl (MMM), Nosztor Limestone, Buhimvölgy Breccia and Csicsó Marl (CsMM) (Figs 2-3) (Budai et al. 1999; Haas et al. 2014) (Fig. 3). The Mencshely Marl consists of grey clayey and calcareous marls with silty, sandy intercalations depending on the contribution from the terrestrial siliciclastic influx and the carbonate mud transported from the surrounding platforms to the basin (Budai et al. 1999; Haas et al. 2014). The Mencshely Marl is followed by a microcrystalline limestone unit of the Nosztor Limestone with radiolarians, planktonic crinoids and sponge spicules indicating deposition in a relatively deep, low energy environment. These carbonate deposits intercalated between the marls are related to platform development in the adjacent areas (De Zanche et al. 1993). The Buhimvölgy Breccia forms the heteropic facies of the Nosztor Limestone and represents the toe of slope sediments within the basin. This member shows lithological similarity to the conglomeratic-breccia deposits known as ”cipit boulder” from the Southern Alps (De Zanche et al. 1993).

In the upper part of the Veszprém Formation, the mixed carbonate-siliciclastic sedimentation returned, represented by marls and calcareous marls of the Csicsó Marl (Figs 2-3). The Veszprém Formation has been correlated to the Heiligkreuz Formation (Dal Corso et al. 2015, 2018) and the Julian part of the Raibler Schichten in the Northern Calcareous Alps (Csillag & Földvári 2005). The source area of pelitic material of the Veszprém Formation could have been in palaeogeographical relation with that of the Val Sabbia Sandstone in the Lombardian continental area (Budai et al. 1999). The Val Sabbia Sandstone is composed of eroded material from the Variscan basement and its Upper Carboniferous–Ladinian sedimentary cover with significant contribution of volcanic detritus (Garzanti 1985; Garzanti & Pagni Frette 1991; Beltrán-Triviño et al. 2016). Consequently, composition of the source area of the fine clastics in the Veszprém Formation could be rather complex.

Ammonoids (*Frankites* sp. and *Trachyceras aon*) and conodonts (*Gladigondollela tethydis, Paragondolella foliata, Paragondolella foliate inclinata*) suggest early Julian age corresponding to the *Trachyceras* ammonoid zone in the underlying Füred Formation (Dosztály et al. 1989; Kovács et al., 1991; Budai et al., 1999). However, *Neoprotrachyceras* spp. and *Sirenites* sp. from the uppermost part of the Füred Formation indicate already the *Austrotrachyceras* ammonoid zone and Julian 2 age (Dal Corso et al. 2015). The age of Veszprém Formation is constrained by ammonite biostratigraphy and the previous palynological studies: *Austrotrachyceras austriacum* is present in the Nosztor Limestone and *Neoprotrachyceras baconicum* in the Csicsó Marl (Budai et al., 1999; Dal Corso et al. 2015) both indicating Julian 2 age. Dal Corso et al. (2015) recorded a significant negative carbon isotope excursion in the lowermost part of the Veszprém Formation form the Balatonfüred-1 borehole in the Balaton Highland area, which was correlated to the characteristic carbon isotope excursion (NCIE-1) marking the onset of the CPE and the Julian 1/2 boundary in the Tethyan realm. Recent $\delta^{13}C_{TOC}$ analyses record the NCIE-1 in the Met-1 section as well between (~ 337-325 m) (Dal Corso et al. 2018). A second NCIE is identified in the upper part of the Met-1 (~135-114 m) (NCIE-2) (Dal Corso et al. 2018).

The palynological assemblages of the Veszprém Formation recovered in previous studies (Góczán et al. 1983, 1991; Góczán & Oravecz-Scheffer 1996a, b) are similar to the *Aulisporites astigmous* assemblage sensu Roghi et al. (2010), characteristic for the Julian 2. The Julian/Tuvalian boundary was placed in the lower part of the overlying Sándorhegy Formation based on previous biostratigraphy (palynology and foraminifers) (Góczán et al. 1983; Góczán & Oravecz-Scheffer 1996a, b) (Fig. 3) although the lack of ammonoids and conodonts can not confirm the biostratigraphic age assignment.

2.2. Carnian succession in the Zsámbék Basin, Gerecse Hills

The encountered Carnian succession of the Gerecse Hills documented in the Zsámbék-14 (Zs–14) is markedly different from the stratotypes in the Balaton Highland-Bakony Mts. (e.g., Haas & Budai 1999, 2014; Budai et al. 2015) (Figs 2-3). Marl layers characteristic for the Veszprém Formation are present only in the lower part of the studied succession. The Mencshely Marl develops continuously from the platform facies of the Budaörs Formation by increasing siliciclastic input (Haas et al. 1981, Haas & Budai 2014). Upsection the marl unit is followed by a cherty limestone unit with marls and subsequently by cherty dolomites of the Csákberény Formation (Figs 2-3). Foraminifers, ostracods and conodont remains indicate a restricted basin environment and poorly oxygenated bottom water conditions (Góczán et al. 1979; Góczán & Oravecz-Scheffer, 1986a, b). An upper marl unit equivalent to the Csicsó Marl is absent. In the Gerecse Hills, the upfilling of the basin ended also in the Tuvalian. Based on the previous palynological and microfossil studies, the Mencshely Marl was assigned to the early Julian. The Csákberény Formation begins in the Julian and extends into the Tuvalian (Góczán et al. 1979; Góczán & Oravecz-Scheffer 1996a). Recently, Dal Corso et al. (2018) recorded a shift to lighter bulk organic carbon isotope ratios in the upper part of the Mencshely Marl (688-686 m) which has been correlated to the NCIE-2 in the Met-1 and other areas of the Alpine Tethys considered to be of late Julian 2 age there. Another negative carbon isotope excursion at the top of the Csákberény Formation is correlated to the NCIE-3 at the Julian/Tuvalian boundary although there is only limited evidence which supports the biostratigraphical age assignment of the Csákberény Formation.

3. Methods

A total of 83 samples were processed for palynological and palynofacies analysis from the three boreholes. The alpha weathering indices (Garzanti et al. 2013) were calculated for 108

samples. The same sample set has been used as in Rostási (2011) and Rostási et al. (2011). Raw data, the description of all laboratory techniques and the summary of the palaeoecological methods are available in Baranyi et al. The palaeoenvironmental interpretation of the palynomorph assemblages is based on the known or presumed botanical and ecological affinity of the dispersed sporomorphs' parent plant. Spore & pollen can be classified as hygrophytic or xerophytic according to the concept of Visscher & Van der Zwan (1981) (see in Baranyi et al.). The Sporomorph Ecogroup Model (SEG) method (Abbink 1998; Abbink et al.2004) has been applied to distinguish plant communities labelled as ecogroups, or SEGs based on the palynomorph content in the samples. In the present study four terrestrial SEGs are distinguished: river SEG, dry and wet lowland SEG and hinterland SEG. The hinterland SEG incorporates pollen from plants growing permanently above groundwater level on well-drained terrains (Kustatscher et al. 2012). The river SEG reflects riverbank communities that are periodically submerged, the dry lowland SEG reflects floodplain vegetation episodically submerged, wet lowland SEG represents marshes and swamps and the hinterland SEG reflects plant communities on well-drained terrains, above groundwater table. The coastal SEG incorporates coastal communities, never submerged but under constant influence of salt spray. Principal component analysis (PCA) was applied to the data set of selected palynomorph groups to display the relationships among the different taxa and reveal the hypothetical (ecological) gradients that influence the variance within the data set (see in Baranyi et al.).

The applied alpha-indices, are based on comparing the concentration of each mobile element to the concentration of an immobile element (Al) with similar magmatic compatibility from the sediment samples. The obtained elemental ratios are then compared to that in the upper continental crust (UCC). For each studied mobile element (E) the normalized value is

calculated as: $\alpha^{Al}_{E} = (Al/E)_{sample}/(Al/E)_{UCC}$. The applied weathering index calculations are the following:

$\alpha^{Al}_{Na} = (Al/Na)sample/(Al/Na)UCC$ (1)

$\alpha^{Al}_{K} = (Al/K)sample/(Al/K)UCC$ (2)

$\alpha^{Al}_{Ba} = (Al/Ba)sample/(Al/Ba)UCC$ (3)

.

4. Results

4.1. Palynology

A total of 55 samples were counted for palynology (Figs 4-5). The samples in the lower part of the Csákberény Formation in the Zs–14 are characterized by the predominance of AOM which prohibited the quantitative analysis. A total of 93 terrestrial taxa and 14 different types of aquatic palynomorphs are distinguished, including freshwater algae and marine palynomorphs. The palynomorphs are generally well preserved, the wall colour varies between pale yellow to golden brown, their SCI index ranges from 2 to 7 depending on wall-thickness variations between the grains (Batten 2002). The palynomorph assemblages throughout are dominated by terrestrial palynomorphs in the studied boreholes. Aquatic palynomorphs and palynofacies patterns are summarized in the Supplementary (Figs S1-S2). In the two boreholes from the Balaton Highland-Bakony (Met-1 and V-1) three local palynological assemblages are distinguished by cluster analysis (CONISS) (Fig. 4). The Mencshely Marl (Met–1 borehole (69.8–373 m, V–1 78–485 m) is dominated by gymnosperm pollen. The *singhii-acutus-vigens* assemblage in the lowermost part of the Mecshely Marl (Met–1/373.9–267.2 m, V–1/549–578) is characterized by the common occurrence of striate (taeniate) bisaccate pollen (*Lunatisporites acutus, Lueckisporites singhii*) (~10-40%) but their abundance decreases towards the top of the Mencshely Marl (up to 10%). The *Alisporites* group (*A. aequalis*) and the Circumpolles, mainly *Partitisporites* (*P.*

novimundanus, *P. tenebrosus*, *P. maljawkinae*) and *Duplicisporites* (*D. continuus*, *D. granulatus*), are also abundant in this assemblage. The abundance *of P. maljawkinae* increases towards the top of the Mencshely Marl from 5-10% to 10-20% in the *acutus-vigens-maljawkinae* assemblage reaching a peak of ~40% at 177.4 m (Met–1/215–69.8 m, V–1/541–485 m). Monosaccate pollen grains are common in both assemblages, represented mainly by *Enzonalasporties vigens* and *Vallasporites ignacii*. The spore taxa form only minor components of the Mencshely Marl palynological assemblages, their proportion is generally low, *ca.* 3–10% of the terrestrial palynomorphs. The most common taxa are laevigate trilete spores (*Calamospora tener*, *Deltoidospora*, *Todisporites* spp., *Dictyophyllidites harrisii*) and *Aratrisporites* spp. *Aulisporites astigmosus* is recorded in both boreholes (first occurrence at 343 m in the Met–1 and at 538–539 m in the V–1) but it is represented only by less than 10 specimens in each sample, mainly 1–2. Towards the top of the Mencshely Marl, the proportion of *A. astigmosus* shows a slight increase in both boreholes. *Lagenella martinii* is recorded first at 299.5 m in the Met–1 and 506 m in the V–1, but this species is very rare in contrast to its frequent occurrence in age-equivalent successions from the "Raibler Schichten" in the Julian Alps or the Lunz area (e.g., Roghi et al. 2010; Muller et al. 2016b).

The *Aratrisporites-astigmosus-densus* local assemblage in the Csicsó Marl (V–1, 353-334.6 m) is characterized by significant increase of spores (up to 40%) and *Aulisporites astigmosus* (5%) (Fig. 4). The most common spore taxa are *Aratrisporites* spp., *Calamospora tener*, *Deltoidospora* sp., *Todisporites major*, *Concavisporites toralis*. Other characteristic taxa are: *Gibeosporites lativerrucosus*, *Uvaesporites gadensis*, *Osmundacidites wellmannii*, *Paraconcavisporites lunzensis*, *Lycopodiacidites kuepperi* and *Camarazonosporites rudis*. Among the monosaccate pollen grains, the abundance of *Patinasporites densus* together with *P. explanatus* and *P. iustus* increases compared to the Mencshely Marl. The bisaccate pollen

grains are mainly represented by the *Alisporites* group, but the assemblage is characterized also by an increase of *Staurosaccites quadrifidus.*

For the topmost part of the Csákberény Formation in the Gerecse Hills (Zs–14 372.2–329.7 m) no local assemblage is defined. The samples are characterized by low spore proportions and the predominance of bisaccate and monosaccate pollen grains (Fig. 5). Spores are represented mainly by *Calamospora tener* and *Deltoidospora* sp. The *Aratrisporites* group occurs only sporadically compared to the high frequency of the group in the Veszprém Formation in the Balaton Highland. Among the bisaccte pollen grains, *Alisporites* spp. are still predominant, but other taxa, e.g., *Ovalipollis* spp. and *Pityosporites* sp., are more common compared to the Veszprém Formation. *Ezonalasporites vigens* and *Vallasporites* are the most frequent species among the monosaccate pollen grains. *Aulisporites astigmosus* is absent.

4.2. Spormorph ecogroups (SEGs)

The application of the SEG method reveals the overall dominance of the hinterland SEG and the dry lowland group. In the lower part of the Mencshely Marl in both cores, the river and wet SEG elements increase in abundance. The Csicsó Marl is characterized by increase in the coastal, riverine and wet lowland SEG elements.

4.3. PCA of terrestrial palynomorphs

The results are displayed as the species scores on the first and second axes of PCA scatter plot (Fig. 6). These two axes can be translated as the two most influential environmental gradients that control the data set (Bonis & Kürschner 2012). The eigenvalues and variance scores (%) give the measure of the variance accounted for by the corresponding environmental component (Harper 1999). The first axis explains 34.2% of the total variance within the data set, the second axis accounts for 26.4% suggesting that axis 1 exerts the principal control on the dataset (Fig. 6). Spores and *Alisporites* have high positive values on axis 1. The *Circumpolles* have high negative values on axis 1. Spores are usually associated with moist

environments (e.g., Abbink et al. 2004; Bonis & Kürschner 2012), and the *Alisporites* group is often assigned to the hygrophytic pollen group (e.g., Whiteside et al. 2015; Mueller et al. 2016a, b). On the contrary, the *Circumpolles* grains produced by the Cheirolepidiaceae are generally indicative of subtropical, tropical drier climate (e.g., Vakhrameev 1991) although the palaeoecological affinity of the group is highly discussed. From the position of the spores relative to the position of *Circumpolles*, axis 1 can be interpreted as a relative humidity gradient, with more humid conditions being indicated by high values of the first principal component. The taeniate pollen (*Lunatisporites*, *Lueckisporites*, *Infernopollenites*) have also positive values on axis 1 representing the humidity gradient. The most abundant element of this group is *Lunatisporites acutus* which has been assigned to the Voltziaceae (Balme 1995; Bonis & Kürschner 2012). The *Circumpolles* have positive values on axis 2 together with spores. Sporomorphs with very high negative values on axis 2 are the taeniate pollen grains (*Lunatisporites*, *Lueckisporites*, *Infernopollenites*). *Vallasporites*, *Enzonalasporites* *Triadispora* and *Ovalipollis* also have negative values on this axis. These palynomorphs are primarily related to conifers e.g., Podocarpaceae, Voltziaceae, Majonicaceae (Balme 1995; Bonis & Kürschner 2012) representing hinterland vegetation elements, while the spores are confined usually to lowland or riverine habitats (Abbink 1998; Abbik et al 2004). The Cheirolepidiaceae, represented by the *Circumpolles* originate from a range of environments including hinterland and dry coastal settings (Batten 1974; Abbink 1998; McArthur et al. 2016; Slater et al. 2017). Due to the strong differentiation between hinterland and lowland (also riverine, coastal) elements, the second principal component on axis 2 might be a function of proximity which distinguishes lowland or coastal vegetation elements and the regional pollen rain.

4.5 Chemical weathering indices

The elements selected to calculate the chemical weathering indices, Al, K, Na and Ba, do not show uniform distribution in the studied sections. The Al and K correlate well with each other both in the Met–1 (r=0.95, R^2=0.91) and V–1 sections (r=0.98, R^2=0.96) suggesting that the distribution of these elements is likely determined by the amount of the aluminosilicate-rich (clay-rich) terrigenous material. In these two core sections, also the elements Al and Ba have positive correlation (r=0.83, R^2=0.69 in Met-1 and r=0.99, R^2=0.97 in V-1) indicating that the concentration of Ba is ultimately controlled by the terrigenous influx. Na has positive correlation with the Al (r=0.82, R^2=0.66 in Met-1, r=0.86 and R^2=0.66 in V-1) which suggests that the concentration of Na is primarily determined by the amount of the terrigenous silicate fraction as well. The same elements behave differently in the case of Zsámbék samples; a correlation coefficient of r=0.86 and R^2=0.74 for Al to Ba is well commensurable to those of the two other sections. However, the low correlation coefficients and low R^2 values (Al/Na r=0.11, R^2= 0.01; Al/K r=-0.09, R^2=0.01) indicate that their concentration changes independently in Zs–14. Consequently, reliable data regarding the chemical weathering indices can be obtained for the Met–1 and the lower part of the V–1 sections. However, interpretation of the weathering proxies from the Zs-14 and the upper part of the V-1 has to be treated with precaution due to the low sampling resolution and the limited stratigraphic extent of the samples.

4.5.1 Met–1 section

Potassium shows moderate mobilization, but the sample at 45.0 m has outstanding high α^{Al}_{K} and α^{Al}_{Ba} values (Fig. 7). The average α^{Al}_{K} is 1.32±0.27 and average α^{Al}_{Ba} has a value of 2.77±1.48 implying that Ba is generally depleted throughout the section relatively to the UCC, but K suffered a moderate degree of impoverishment. The upper part of the Met–1 section (33.8 to 63.0 m) shows drastic fluctuations and usually higher values compared to the samples

from 69.8 to 373.9 m (Fig. 7). The values of the α^{Al}_{Na} index indicate a significant depletion relative to the UCC (Upper Continental Crust) in the samples from 33.8 to 63.0 m with local maxima at 49.4 m and 63.0 m (Peaks of the α^{Al}_{K} and α^{Al}_{Ba} values are recorded at 49.4 (2.27 and 7.57 respectively) and at 63.0 m (2.37 and 8.12 respectively). Slightly elevated α^{Al}_{K} indices can be observed in the depth interval of ~177.4 to 255.5 m; this pattern can be traced in the α^{Al}_{Ba} curve as well but it cannot be seen in the curve of the α^{Al}_{Na} indices which forms a characteristic bow-like pattern with minima in this interval.

4.5.2. V–1 section

The α-indices show a net but varying degree of depletion regarding the Na and Ba with average values of 8.29±4.08 and 3.00±0.97 (Fig. 7). However, the K with its average of 0.99±0.18 seems not to be mobilized from the studied V–1 samples. This general difference between the rate of the mobilization (with an order of Na>Ba>K) is rather similar to that of the Met–1 section (Fig. 7). The V–1 and Met–1 sections are rather similar regarding the α-indices pattern: the Ba and K have almost the same character but the Na has different one (Fig. 7). The deeper part of the succession representing the Mencshely Marl (from 485.0 to 591.0 m) shows hectic fluctuations with four distinct peaks (at 486.0, 544.0, 560.5 and 591.0 m) and a general decreasing upward trend both on the α^{Al}_{Ba} and α^{Al}_{K} curves. Contrarily, the α^{Al}_{Na} values are organized to another pattern with a minimum at 523.2 m. The index increases both downsection and upsection from this reference point with an extremely high value in the deepest sample from the core (591.0 m). In spite of the limited number of the studied samples, interesting trends are outlined in the Csicsó Marl. The samples from 336.0 to 364.0 m of the V–1 section show an almost parallel run for the α^{Al}_{Ba} and α^{Al}_{K} curves but the Na behaves differently. Both α^{Al}_{Ba} and α^{Al}_{K} curves have the highest value at the depth of 364.0 m and two additional maxima at 352.0 and 338.0 m. The in α^{Al}_{Na} indices show a decreasing trend in the

Csicsó Marl with elevated values (12.76–17.75) between 352.0 and 364.0 m decreasing towards the top of the studied interval.

4.5.3. Zs–14 section

The α-indices for the potassium from the Zs–14 indicate a net enrichment with values <1, excluding the samples from the 327.0 to 352.0 m depth interval, and display a quite fluctuating pattern (Fig. 7). Contrarily, the Ba suffered a pronounced depletion with average α^{Al}_{Ba} values of 6.23±3.20. The sodium behaves differently in the two formations represented in the core Zs–14: the Mencshely Marl (678.0–754.5 m depth) is characterized by a very moderate degree of depletion (average α^{Al}_{Na} = 1.30±0.27), the α^{Al}_{Na} of the Csákberény Formation (320.5–386.5 m depth) fluctuates between 1.94 and 33.76 suggesting a rather elevated sodium mobilization.

It is noteworthy that, contrarily to the two other studied sections, the α^{Al}_{Na} and α^{Al}_{K} curves have a similar path. Three maxima seem to be outlined in the Mencshely Marl at the interval of 690–710 and at the depth of 741.5 and 734.0 m. The depth interval of 327.0–352.0 m of the Csákberény Formation shows increased values relatively to the two neighbouring parts of this formation in the Zs–14 section (Fig. 7).

5 Discussion

5.1. Palynostratigraphy and correlation

The palynological assemblages and selected palynomorph events can be used to correlate the sections with other successions from the Western Tethys. The studied assemblages within the lower Veszprém Formation can be correlated to the Julian 2 *Aulisporites astigmosus* assemblage of Roghi et al. (2010), the lower part of the *Duplicisporites continuus* assemblage of Roghi (2004) and based on the co-occurrence of *Aratrisporites* and *Aulisporites*, to the *Aulisporites-Aratrisporites acme* (Roghi 2004). *Duplicisporites continuus* is present from the base of both boreholes in the Balaton Highland (Figs 3-4). *Aulisporites astigmosus* was first

recorded close to the base of the studied intervals and is present throughout the Veszprém Formation from at the depth 343 m in the Met–1 and 538–539 m in the V–1 (Figs 3-4). Based on the common occurrence of *Patinasporites densus* and *Partitisporites maljawkinae*, the assemblages in the Balaton Highland correspond also to the *densus-maljawkinae phase* of Van der Eem (1983). The *Lagenella martinii* assemblage (Roghi et al. 2010) cannot be recognized in the studied successions from the TR, as the species is very rare in the studied samples. The local first occurrence of the species in recorded at depth 299.5 m in the Met–1 and 506 m in the V–1 within the Mencshely Marl (Figs 3-4). It has been reported by Góczán et al. (1983) from the Hévíz–6 core (Keszthely Mts, SW part of the TR) in the Csicsó Marl in an *Aratrisporites-Saturnisporites* dominated assemblage. However, other characteristic elements of the *Lagenella martinii* assemblage (e.g., *Aratrisporites, Concavisporites, Calamospora, Lycopodiacidites kuepperi, Patinasporites densus*) from the "Raibler Schichten" (Kavary 1966; Jelen & Kušej 1982; Roghi et al. 2010) or Lunz area are recorded from the studied interval of the Csicsó Marl in the V–1.

The Julian/Tuvalian boundary was previously placed in the lower part of the overlying Sándorhegy Formation in the Balaton Highland and in the upper part of the Csákberény Formation in the Gerecse Hills (Góczán & Oravecz-Scheffer 1996a, b; Haas & Budai 2014). Góczán & Oravecz-Scheffer (1996a, b) considered the first local appearance of *Pseudoenzonalasporites summus* within the Sándorhegy Formation and the upper part of the Csákberény Formation (previously also named as Sándorhegy Formation) as the indicator of the Tuvalian substage. However, the species is present already from the early Carnian in the Northern Hemisphere (e.g., Cirilli 2010). Conodonts from the Zs-14 cannot pinpoint the Julian/Tuvalian boundary and the Tuvalian age for the topmost Csákberény Formation is only supported by the foraminifer assemblage (Kristan-Tollmann et al. 1991). The palynological assemblage recorded in the upper part of the Zs–14 is not age-diagnostic; it is not possible to

assign it to any substage with certainty. Already, Góczán & Oravecz-Scheffer (1996a, b) pointed out the lack of the characteristic Tuvalian taxa e.g., *Ricciisporites tuberculatus* or *Granuloperculatipollis rudis* in this assemblage. *Kyrtomisporis ervii* was a characteristic element of the spore assemblage in this interval (Góczán & Oravecz-Scheffer 1996a, b and this study), although this species is present only in the early Carnian (Julian 1) palynological assemblages in the Dolomites (Roghi 2004). *Aulisporites astigmosus* is absent. The lack of the species is not age-diagnostic, but it is already absent in the Tuvalian according to the NW European palynological zonations (Kürschner & Herngreen 2010) and it has not been found in any other presumed Tuvalian assemblages of the TR (Góczán & Oravecz-Scheffer 1996a, b).

5.2. Palaeoenvironmental implications of the palynological assemblages

A significant feature of the TR palynological assemblages is the predominance of hinterland elements i.e. conifer pollen (Figs 8-9). Spores reach a greater abundance in the Dolomites, Julian Alps, the "Raibler Schichten" or the Lunz Formation (Planderová 1980; Blendinger 1988; Roghi 2004; Roghi et al. 2010; Mueller et al. 2016b) than in the TR. The parent plants of the conifer pollen grains are considered to be overproducers and their pollen have the ability to be transported by wind over great distances (hundreds of kilometres), while spores are more common in nearshore proximal settings (e.g., Chaloner & Muir 1968; Vakhrameev 1991; McArthur et al. 2016). The TR was located in a relatively more distal depositional setting at the start of the CPE compared to the Northern Calcareous Alps, Julian Alps or the Dolomites (Haas & Budai 1995). During the Carnian, the Dolomites and Northern Calcareous Alps recorded a transition from basinal setting to shallow carbonate-clastic shelf including prodelta environments (e.g., Lunz Formation in Dal Corso et al. 2015), while in the TR, the Veszprém Formation and the overlying Sándorhegy Formation represents the transition from hemipelagic basin to shallow carbonate shelf without a delta/prodelta series (Budai & Haas 1997; Budai et al. 1999; Haas & Budai 1999). Same shallow carbonate platform

environmental conditions developed first in the late Tuvalian in the three areas (Dolomites, Northern Calcareous Alps and the TR) with the formation of the Main Dolomite (Haas & Budai 1995; Haas et al. 1995).

5.3. Climate change in the Transdanubian Range during the CPE

In the TR, the clay mineral record of Rostási et al. (2011) extended with weathering indices and the presented palynological data provide two independent climate proxies which clearly indicate distinct climatic variations during the CPE. The clay mineral profile of the Carnian formations in the TR consists mainly of illite, mixed-layer illite/smectite and to a lesser extent kaolinite and chlorite with a significant increase in kaolinite in the Veszprém Formation (Rostási et al. 2011). In the underlying formations, the Füred Formation in the Balaton Highland and in the Budaörs Formation in the Gerecse Hills, kaolinite is absent (Viczián 1995; Rostási et al. 2011) suggesting a significant change in clay mineral composition during the Julian 2. An increase in kaolinite abundance in the clay mineral composition is a good marker for weathering of landmasses with good drainage under a hot and humid (subtropical, tropical) climate (e.g., Ruffel et al. 2002; Raucsik & Varga 2008; Dera et al. 2009; Branski 2010; Rostási et al. 2011).

In the Mencshely Marl in the Met–1 two intervals, 325.9–260 m and 150–69 m are characterized by higher hygrophytic/xerophytic ratio and an increase in the wet lowland and riverine SEG elements suggesting the expansion of wet habitats on the continent (Fig. 8). The relative humidity gradient reconstructed by PCA (PCA 1 axis) also indicates relatively more humid conditions for the intervals of 325.9–260 m and 150–69 m (Fig. 8). The higher kaolinite ratio in the clay mineral record in 373.9-260 m and 90-69 m would also suggest increased weathering rates. The calculated α-indices show a general depletion of the mobile elements relatively to the UCC. The depth interval of 33.8 to 63 m of the Met–1 section obtains high αAl_{Na} values with drastic fluctuations of chemical weathering indices which

might attest dramatic changes and elevated degree of continental hydrolysis relatively to the deeper part of the Mencshely Marl in the Met–1 section. The slightly elevated αAl_K values and less pronouncedly the αAl_{Ba} indices in the lower part of the Mencshely Marl in the depth interval of ~177.4 to 255.5 m (Fig. 7) can also be a consequence of enhanced runoff related to a more humid climate excursion.

Similar palynological and geochemical trends are observed in Mencshely Marl within the V–1 in the intervals 549–527 m and in the uppermost part of the Mencshely Marl between 501 m and 485 m (Fig. 8). The shift to relatively more humid conditions is also suggested for these intervals by the humidity gradient of the PCA. Like in the Met–1, the hectic fluctuations of the α^{Al}_{Ba} and α^{Al}_{K} curves with several distinct peaks in the V–1 (at 486, 544, 560.5 and 591 m) might indicate changes in the continental weathering rate which was probably more pronounced in the lower part of the Mencshely Marl .The kaolinite ratio is strongly fluctuating within the Mencshely Marl in both borehole sections (Fig. 8).

Rostási et al. (2011) explained this variation in the clay mineralogy as the consequence of the complex basin topography, ocean current patterns and a rift and graben systems that were intermittently active through a time of assumed palaeoclimate changes. Besides climate and palaeotopography, provenance influences the terrestrial material transported into the marine basins and it might alter the recorded alpha values. The clastic influx in the Veszprém Marl Formation had a rather complex source material with heterogeneous origin. The heterogeneity of the terrestrial input can significantly influence the chemical composition of sandy sediments, yet it affects only moderately the bulk chemistry of clay-rich muds (Garzanti & Resentini 2016; Schneider et al. 2016).

The palynological assemblages from the Mencshely Marl from the Gerecse Hills (Zs–14) could not be studied due to the predominance of AOM. Nevertheless, the high kaolinite content indicates enhanced runoff also in that basin of the TR (Rostási et al. 2011). The

drastic variations in weathering indices imply significant changes in the weathering regime; however, the increase in the continental hydrolysis was significant mainly in the lower part of the Mencshely Marl suggested by α-values like those in the V–1.

The deposition of various carbonate units between the Mencshely and Csicsó Marl (e.g., Nosztor Limestone, Sédvölgy Dolomite) within the Julian 2 in the TR is related to the highstand progradation of the carbonate platforms and the decrease of the siliciclastic influx (Budai & Haas 1997; Haas & Budai 1999). The clay mineral composition of these units shows a decrease in kaolinite abundance (Rostási 2011) indicating perhaps a drier episode with the decrease of the continental hydrolysis. Carbonate units are also present in the Dolomites, Julian Alps and Northern Calcareous Alps between the siliciclastic pulses assigned to drier periods (Roghi et al. 2010).

In the late Julian 2, the quantitative analysis of the palynomorph assemblages shows a significant increase in the hygrophytic elements and increase in the riverine and wet lowland SEG elements in the Csicsó Marl (Fig. 8). In agreement with the presented data, the previous palynological studies recorded an *Aratrisporites-Saturnisporites* dominated assemblage with the permanent occurrence of *Aulisporites astigmosus* in the Csicsó Marl (from a ca. 130 m long interval inthe Hévíz–6 borehole) (Góczán et al. 1983) which suggests the constant presence of hygrophytic vegetation during its deposition. The composition of the palynoflora indicates a lowland-riverine vegetation with ferns, lycopsids and Bennettitales similar to that known from e.g., the Lunz flora (Bharadwaj & Singh 1964; Pott et al. 2018; Roghi et al. 2010; Mueller et al. 2016b).

The α values are heavily fluctuating in the Csicsó Marl. Both the α^{Al}_{Ba} and α^{Al}_{K} curves reach their highest value at the depth of 364.0 m followed by two additional maxima at 352.0 and 338.0 m. The αAl_{Na} index curve begins with extremely high values of 12.76–17.75 in the depth interval of 352.0 to 364.0 m and drop to lower but relatively high values (6.65–7.20) of

the samples from 336.0 to 348.0 m (Fig. 7). These features in combination with palynology would suggest a second humid episode which is also corroborated by the trend in the humidity gradient of the PCA (Fig. 8). However, the trends of the α curves have decreasing tendency and the kaolinite ratio is surprisingly low in this interval compared to the Mencshely Marl (Fig. 8). In the clay mineral record, the abundance of mixed-layer illite/smectite is higher in this interval compared to the Mencshely Marl (Rostási 2011), which perhaps suggests a more pronounced seasonality (Ruffell et al. 2002).

In general vegetation contributes significantly to weathering processes (e.g., Egli et al. 2008). However, on long-term, vegetation can improve soil physical properties and anti-erodibility; reduce runoff and erosion (e.g., Zhang et al. 2015). Perhaps the dense lowland vegetation in the nearby coastal area reflected by the palynological assemblage in the Csicsó Marl trapped some of the sediment influx into the marine basin affecting also the clay mineral record. Besides climate, sea level variations can be accounted as well for the observed palynological record. The increase in Bennettitales, ferns and lycophytes in the Csicsó Marl can be related to sea level drop in the late Julian 2 (Haas & Budai 1999; Csillag & Földvári 2005), the progradation of fluvio-deltaic environments and increased input of the terrestrial plant material from the nearby coastal areas.

The last interval with enhanced siliciclastic input within the Carnian is documented in the Tuvalian, in the upper part of the Sándorhegy Formation (Barnag Member) (Balaton Highland-Bakony Mts.) and in the uppermost part of the Csákberény Formation in the Gerecse Hills (previously also Sándorhegy Formation, Barnag Member) (Fig. 9). However, the palynological assemblage from the upper part of the Csákberény Formation in the Zs–14 is represented mainly by gymnosperms pollen assigned to the xerophytic group (*Vallasporites ignacii*, *Enzonalasporites vigens, Circumpolles*). The terrestrial influx in this interval is perhaps related mainly to sea level changes, as there is no indication for a widespread

hygrophytic vegetation and humid climate. The same palynological trend is observed in the last siliciclastic horizon of the "Raibler Schichten" (Kavary 1966, 1972; Jelen & Kušej 1982; Roghi et al. 2010) where the xerophytic pollen types are predominant in the palynology. The increase in xerophytic pollen was explained as a return to drier climatic conditions in the area of the Western Tethys later in the Carnian and Norian (Roghi et al. 2010). The clay mineral composition from the uppermost part of the Zs–14 in the Gerecse Hills shows a decrease in the kaolinite content which might be related to the decrease in the weathering intensity and drier climate during the early Tuvalian (Rostási et al. 2011) (Fig. 9) In addition, clay mineral data from an outcrop of the age-equivalent Sándorhegy Formation in the Balaton Highland (Nosztor Valley, Csopak) indicate the predominance of illite and weathering under arid to semi-arid conditions (Raucsik et al. 2005). The potassium distribution in the upper part of the Zs-14 is not discussed because of higher degree of diagenetic overprint proven by expandability of the mixed-layer illite/smectite (Rostási et al. 2011). This diagenetic K-uptake might be resulted in the net enrichment with values <1, excluding some samples from the horizon of 327.0 to 352.0 m (Fig. 7). The other studied α-indices from the Zs–14 section fluctuate in a rather hectic manner but they show similar trend. It is noteworthy that the depth interval of 327.0–352.0 m shows increased α^{Al}_{Na} and α^{Al}_{K} values relatively to the two neighbouring parts of the Csákberény Formation in the Zs–14 section (Fig. 7) which might be the result of a short increase in intensity of hydrolysis but probably within a generally drier prevailing background climate.

5.5. Correlation of the siliciclastic intervals from the TR to the western Tethys

Three to four clastic intervals intercalated between carbonate units can be distinguished in the Carnian stratigraphic successions of the western Tethys which coincide with the four negative carbon isotope excursions related to multiple injection of ^{13}C depleted carbon into the ocean-

atmosphere (Dal Corso et al. 2018) (Fig. 10). These clastic intervals are assumed to be linked to discrete episodes of more humid climate and enhanced hydrological cycle (Roghi et al. 2010; Stefani et al. 2010; Dal Corso et al. 2018). The first terrigenous pulse is recorded at the base of the Borca Member in the lower Heiligkreuz Formation in the Dolomites coinciding with the first NCIE at the Julian 1/Julian 2 boundary. This pulse is only recorded in basin successions according to Roghi et al. (2010). The palynological assemblage of the first pulse is characterized by the presence of *Aulisporites astigmous* and *Duplicisporites continuus* in the Dolomites and Julian Alps (Roghi 2004). In the TR, *A. astigmous* and *D. continuus* are present in the lower part of the Mencshely Marl in both boreholes from the Balaton Highland-Bakony Mts (V–1 and Met–1) suggesting that this unit most likely corresponds to the first siliciclastic pulse within the Tethyan realm. A similar palynological assemblage is known from the Reingraben Formation in the Lunz area (Roghi et al. 2010; Mueller et al. 2016b) that also marks the switch from carbonate to siliciclastic-dominated sedimentation in the Northern Calcareous Alps. A negative carbon isotope excursion at Lunz beginning in the topmost part of the Reifling Formation and extending into the Göstling Member and Reingraben Formation can be correlated to the NCIE-1 of Dal Corso et al. (2018) (Fig. 10) connecting the Reingraben Formation to the first clastic pulse from the Dolomites.

The second siliciclastic pulse is located in the lower part of the Dibona Member in a higher stratigraphical part of the Heiligkreuz Formation in the Dolomites and in the first shale of the "Raibler Schichten" in the Northern Calcareous Alps (Roghi et al. 2010) linked to NCIE-2. The third pulse is located in the lower part of the Lagazuoi Member in the uppermost part of the Heiligkreuz Formation and in the second shale of the "Raibler Schichten" associated with NCIE-3. Both pulses are characterized by a palynological assemblages with the predominance of hygrophytic spore-pollen types e.g., the *Aratrisporites* group, laevigate trilete spores (*Calamospora* spp., *Concavisporites*), *Aulisporites astigmosus*, *Cycadopites* sp.,

Lycopodiacidites kuepperi and *Lagenella martinii*, but the second pulse differs due to the abundance of the pollen *Patinasporites densus* in the first shale of the "Raibler Schichten" (Roghi et al. 2010). A similar palynological assemblage with high amount of spores and *P. densus* has been recorded from the Csicsó Marl in the TR but the first increase in spores is already recorded at the top of the Mencshely Marl. The increase in these palynomorphs suggests that the top of the Mencshely Marl and the Csicsó Marl might correlate to the second and probably third clastic pulses, but they cannot be exactly matched with those in the Dolomites. Discrete clastic pulses separated by carbonates are missing from the Lunz Formation in the Northern Calcareous Alps which is characterized by predominantly clastic deposition during the whole Julian 2.

The fourth siliciclastic pulse is recorded at the base of the Travenanzes Formation in the Tuvalian 2 in the Dolomites and in the third shale of the "Raibler Schichten" (Roghi et al. 2010). The characteristic palynological assemblage of this pulse includes *Vallasporites ignacii*, *Enzonalasporites vigens*, *Circumpolles* especially *Granuloperculatipollis rudis* and *Riccisporites* (Roghi et al. 2010). In the TR, similar palynological assemblage is recovered from the upper part of the Sándorhegy Formation (Barnag Member) in the Balaton Highland-Bakony Mts area (Góczán & Oravecz-Scheffer 1996 a, b) and the uppermost part of the Csákberény Formation in the Zs-14 (this study). Unfortunately, the age of the Csákberény Formation in the Zs–14 is not well constrained biostratigraphically. The corresponding NCIE at the top of the Csákberény Formation was correlated to the NCIE-3 at the Julian/Tuvalian boundary by Dal Corso et al. (2018).

5.4. The CPE is not uniform

The biotic and environmental changes during the CPE are traditionally linked to multiple intervals with humid climatic conditions (e.g., Simms & Ruffell 1989, 1990; Roghi et al.

2010). Yet the nature of the CPE is still widely debated and it appears to be heterogeneous with marked differences in the intensity of the climate change regionally. The question arises whether the CPE is truly humid or it is probably related to the one-dimensional interpretation of certain climate proxies e.g., hygrophytic/xerophytic ratio from the palynology. The recorded increase in the sporomorphs with hygrophytic affinity during the CPE can be explained by increased rainfall and runoff. However, sea level variations and the progradation of the terrestrial facies into marginal marine settings can also account for the observed increased terrestrial input. Moreover, taphonomy, transport mechanisms and the differences in spore/pollen production rates of the plants can alter the composition of the palynological assemblages therefore the climatic interpretation might be biased (e.g., Baranyi et al. 2018). In the TR the increase in hygrophytic elements in the palynological assemblages coincides with elevated kaolinite proportions and the weathering proxies suggest variations in the continental hydrolysis. The combination of these palaeoclimate proxies can confirm the proposed humid climate and enhanced hydrological cycle on the continents adjacent to the Western Tethys realm for the early Julian 2. An additional common feature of these clastic Carnian deposits of the Western Tethys is the occurrence of amber remains in marginal marine settings e,g,, in the Heiligkreuz Formation, Lunz Formation, Sándorhegy Formation and Rio del Lago Formation (Csillag & Földvári 2005; Roghi et al 2006; Seyfullah et al. 2018). More resin is produced under wetter climatic conditions (Langenheim 2003) but increased resin production can also be linked to environmental stress e.g., SO_2 poisoning, wildfires, increased storminess that are related to volcanic activity and higher pCO_2 levels (Seyfullah et al. 2018). The contemporaneous appearance of amber droplets across the Western Tethys during the CPE indicates similar climate evolution in this area and the vegetation likely responded to the same environmental changes corroborated by the similarity of the palynological assemblages as well.

However, climate proxies from the UK (palynology, Baranyi et al. 2018) and Spain (clay mineralogy, Barrenecha et al. 2018) indicate more humidity that stand out only compared to the arid Late Triassic but these data do not point to markedly increased rainfall. Some studies even negate a Carnian climate change: Visscher et al. (1994) argued against the shift to humid climate based on only the palynological assemblages from the Schilfsandstein in the Germanic Basin and suggested that the increase in hygrophytic vegetation elements has only local extent. Recently, Franz et al. (2018) proposed a new coupled model between climate and sea-level changes that explains the local expansion of the hygrophytic flora in the Schilfsandstein similarly to the interpretation of Visscher et al. (1994). This latter model suggests that a eustatic sea level rise resulted in increased evaporation in the basin and increased precipitation over the surrounding hinterland, leading to elevated ground water stages on the floodplains. The local wet habitats established favourable conditions for an intrazonal hygrophytic flora with Bennettitales, ferns and lycophytes while low maturity Carnian sandstones, clay mineral profiles and paleosols indicative of high evaporation rates suggest a prevailing arid, semi-arid background climate with low chemical weathering (Franz et al. 2018).

5.4.

6 Conclusions

The sedimentation of the mixed carbonate-siliciclastic series of the Veszprém Formation during the late Julian-early Tuvalian of the Transdanubian Range indicates increased terrestrial input into the sedimentary basin. The change in depositional style in the late Julian is known from other areas of the Western Tethys and is linked to a humid climatic interval, the Carnian Pluvial Episode (CPE). Palynological assemblages and elemental weathering proxies have been applied to track climate during the CPE. The increase in the hygrophytic

vegetation elements is coincident with elevated kaolinite values and partially with the increase of α-indices indicating strong terrestrial runoff and enhanced continental hydrolysis in lower part of the Veszprém Formation (Mencshely Marl) in agreement with the proposed climate change with increased rainfall in the early Julian 2 The upper marl unit of the Veszprém Formation (Csicsó Marl) points to the renewal of the siliciclastic influx and the high amount of hygrophytic spore and pollen in the palynological assemblages point to a second humid episode. However, the comparison to clay mineralogy suggests stronger seasonality and diminished continental weathering despite the rise in the hygrophytic palynofloral elements. The increase in these lowland vegetation elements generally associated with hygrophytic affinity and wet habitats can be also linked to sea level change during the Julian 2and the progradation of the terrestrial facies into marginal marine settings. . The palynological assemblage from the upper part of the Csákberény Formation consisting of predominately xerophytic pollen types together with the low kaolinite values suggest the return to drier climate in the Tuvalian.

Discrete clastic pulses documented in other areas of the western Tethys can be recognized in the Carnian succession of the TR as well. Three intervals are distinguished: the lower part of the Mencshely Marl correlates to the first clastic episode known from the Dolomites and Julian Alps (Roghi et al. 2010). The top of the Mencshely Marl and the Csicsó Marl probably include both the second and third pulses but they cannot be separated in the TR and matched exactly with the clastic pulses from the Dolomites. The last interval with enhanced terrestrial input is located in the upper part of the Tuvalian Sándorhegy Formation in the Balaton Highland-Bakony Mts. and the upper part of the Csákberény Formation in the Gerecse Hills from the early Tuvalian.

The variations between wetter and drier episodes proposed for the CPE by Roghi et al. (2010) were also present in the TR. Episodes with enhanced terrigenous influx and sedimentation of

marls were interrupted by the highstand progradation of carbonate platforms. Although the clastic pulses in the western Tethys were related to discrete humid climatic episodes (except the fourth pulse), the comparison to clay mineralogy and weathering proxies suggests a more complicated scenario in the TR. The clay mineral and palynological records can be influenced also by other environmental parameters e.g., sea level variations, basin topography or provenance. The enhanced continental weathering related to a more humid climate is only suggested for the lower part of the Veszprém Formation, the Mencshely Marl in the early stage of the CPE in the Julian 2.

Acknowledgements

WMK and VB acknowledge funding from the Faculty of Mathematics and Natural Sciences at the University of Oslo (Norway). Mufak Said Naoroz (UiO) is thanked for his help in the processing of the palynological samples. We thankfully acknowledge the help of János Haas on a fieldtrip in the Transdanubian Range. Steven Mueller helped with the sampling. Two anonymous reviewers are thanked for the thorough reviews and constructive comments, which helped to improve the paper.

Data Availability

Supplementary information to this article can be found online at: Data are available in Baranyi et al.

References

Abbink, O.A., 1998. Palynological investigations in the Jurassic of the North Sea region. Ph.D. Thesis, University of Utrecht, Netherlands.

Abbink, O.A., van Konijnenburg-van Cittert, J.H.A., Visscher, H., 2004. A sporomorph ecogroup model for the Northwest European Jurassic - Lower Cretaceousi: concepts and framework. Neth. J. Geosci.-Geol. En Mijnb, 83, 17–31, https://doi.org/10.1017/S0016774600020436

Balini, M., Lucas, S.G., Jenks, J.F., Spielmann, J.A., 2010. Triassic ammonoid biostratigraphy: an overview. Geological Society, London, Special Publications 334, 221–262, http://dx.doi.org/10.1144/SP334.10

Balme, B.E., 1995. Fossil in situ spores and pollen grains: an annotated catalogue. Rev. Palaeobot. Palynol 87, 81–323, https://doi.10.1016/0034-6667(95)93235-X

Baranyi, V., Miller, C.S., Ruffell, A., Hounslow, M.W., Kürschner, W.M. 2018. A continental record of the Carnian Pluvial Episode (CPE) from the Mercia Mudstone Group (UK): palynology and climatic implications. Journal of the Geological Society, 176, 149–166, https://doi.org/10.1144/jgs2017-150

Baranyi, V., Rostási, Á., Raucsik, B., Kürschner, W.M. Palynology and inorganic geochemistry of Carnian (Late Triassic) formations from the Transdanubian Range (western Hungary). Data in Brief

Barrenechea, J.F., López-Gómez, J., De La Horra, R., 2018. Sedimentology, clay mineralogy and palaeosols of the Mid-Carnian Pluvial Episode in eastern Spain: insights into humidity and sea-level variations. Journal of the Geological Society, in press, https://doi.org/10.1144/jgs2018-024

Batten, D.J., 1974. Wealden palaeoecology from the distribution of plant fossils. Proceedings of the Geologists' Association 85, 433–458, https://doi.org/10.1016/S0016-7878(74)80068-4

Batten, D.J., 2002. Palynofacies and petroleum potential. In: Jansonius, J., McGregor, D.C., (Eds.), Palynology: Principles and Applications. American Association of Stratigraphic Palynologists Foundation, 3, 1065–1084.

Beltrán-Triviño, A., Winkler, W., von Quadt, A., Gallhofer, D., 2016. Triassic magmatism on the transition from Variscan to Alpine cycles: evidence from U–Pb, Hf, and geochemistry of detrital minerals. Swiss Journal of Geosciences, 109/3, 309–328, https://doi.org/10.1007/s00015-016-0234-3

Benton, M.J., Bernardi, M., Kinsella, C. 2018. The Carnian Pluvial Episode and the origin of dinosaurs. Journal of the Geological Society, in press, http://dx.doi.org/10.1144/jgs2018-049

Bernardi, M., Gianolla, P., Petti, F.M., Mietto, P., Benton, M.J., 2018. Dinosaur diversification linked to the Carnian Pluvial Episode. Nat. Comm. 9, 1499, https://doi.org/10.1038/s41467-018-03996-1

Bharadwaj, D.C. & Singh, H.P., 1964. An Upper Triassic miospore assemblage from the Coals of Lunz, Austria. Palaeobotanist 12, 28–49.

Blendinger, E., 1988. Palynostratigraphy of the late Ladinian and Carnian in the Southeastern Dolomites. Rev. Palaeobot. Palynol 53, 329–348, https://doi.org/10.1016/0034-6667(88)90038-3

Bonis, N.R. & Kürschner, W.M., 2012. Vegetation history, diversity patterns, and climate change across the Triassic/Jurassic boundary. Paleobiology 38, 240–264, https://doi.org/10.1666/09071.1

Branski, P., 2010. Kaolinite peaks in early Toarcian profiles from the Polish Basin - an inferred record of global warming. Geological Quarterly 54, 15–24

Breda, A., Roghi, G., Furin, S., Meneguolo, R., Ragazzi, E., Fedele, P., Gianolla, P., 2009. The Carnian Pluvial Event in the Tofane area (Cortina d'Ampezzo, Dolomites, Italy). Geo.Alp, 6, 80–115.

Budai, T., Haas, J., 1997. Triassic sequence stratigraphy of the Balaton Highland, Hungary. Acta Geol. Hung. 40, 307–335.

Budai, T., Császár, G., Csillag, G., Dudko, A., Koloszár, L., Majoros, Gy., 1999. Geology of the Balaton Highland (Explanation to the Geological Map of the Balaton Highland, 1:50000). Special Publications of the Geological Institute of Hungary 197, 171–257.

Budai, T., Piros, O., Haas, J., 2015. Új rétegtani adatok a Zsámbéki-medence triász aljzatából – szerkezetföldtani következtetések. Földtani Közlöny, 145, 247–257, (in Hungarian, with English Abstr.)

Budai, T., Vörös, A., 2006. Middle Triassic platform and basin evolution of the Southern Bakony Mountains (Transdanubian Range, Hungary). Rivista Italiana di Paleontologia e Stratigrafia, 112, 359–371, https://doi.org/10.13130/2039-4942/6346

Chaloner, W.G., Muir, M. 1968. Spores and floras. In: Murchison, D.G., Westoll, T.S. (Eds.), Coal and coal-bearing strata. Oliver and Boyd, Edinburgh, 122–146.

Chen, Y, Krystyn, L., Orchard, M.J., Lai, X.-L., Richoz, S., 2015. A review of the evolution, biostratigraphy, provincialism and diversity of Middle and early Late Triassic conodonts. Papers in Palaeontology, 2, 235–263, http://dx.doi.org/10.5061/dryad.34r55

Cirilli, S., 2010. Upper Triassic–lowermost Jurassic palynology and palynostratigraphy: a review. In: Lucas, S.G. (Ed.), The Triassic Timescale. Geological Society, London, Special Publications, 334, 285–314, https://doi.10.1144/SP334.12

Csillag, G., Földvári, M., 2005. Felső-triász gyantatöredék a Balaton-felvidékről. Magyar Állami Földtani Inézet Évi Jelentése 2005-ről, 37–46, (in Hungarian, with English Abstr.)

Csontos, L., Nagymarosy, A., Horváth, F., Kovác, M., 1992. Tertiary evolution of the Intra-Carpathian area: a model. Tectonophysics 208, 221–241, https://doi.org/10.1016/0040-1951(92)90346-8

Csontos, L., Vörös, A., 2004. Mesozoic plate tectonic reconstruction of the Carpathian region. Palaeogeography, Palaeoclimatology, Palaeoecology 210, 1–56, https://doi.org/10.1016/j.palaeo.2004.02.033

Dal Corso, J., Gianolla, P., Newton, R.J., Franceschi, M., Roghi, G., Caggiati, M., Raucsik, B., Budai, T., Haas, J., Preto, N., 2015. Carbon isotope records reveal synchronicity between

carbon cycle perturbation and the "Carnian Pluvial Event" in the Tethys realm (Late Triassic). Global and Planetary Change 127, 79–90, https://doi.org/10.1016/j.gloplacha.2015.01.013

Dal Corso, J., Gianolla, P., Rigo, M., Franceschi, M., Roghi, G., Mietto, P., Manfrin, S., Raucsik, B., Budai, T., Jenkyns, H.C., Reymond, C.E., Caggiati, M., Gattolin, G., Breda, A., Merico, A., Preto, N., 2018. Multiple negative carbon-isotope excursions during the Carnian Pluvial Episode (Late Triassic). Earth-Science Reviews, 185, 732–750, https://doi.org/10.1016/j.earscirev.2018.07.004

Dal Corso, J., Mietto, P., Newton, R.J., Pancost, R.D., Preto, N., Roghi, G., Wignall, P.B., 2012. Discovery of a major negative $\delta^{13}C$ spike in the Carnian (Late Triassic) linked to the eruption of Wrangellia flood basalts. Geology, 40, 79–82, https://doi.10.1130/G32473.1

Dal Corso, J., Ruffell, A., Preto, N., 2019. Carnian (Late Triassic) C-isotope excursions, environmental changes, and biotic turnover: a global perturbation of the Earth's surface system. Journal of the Geological Society, *in press*, *https://doi.org/10.1144/jgs2018-217*

Dera, G., Pellenard, P., Neige, P., Deconinck, J.-F., Pucéat, E., Dommergues, J.-L., 2009. Distribution of clay minerals in Early Jurassic Peritethyan seas: Palaeoclimatic significance inferred from multiproxy comparisons. Palaeogeography, Palaeoclimatology, Palaeoecology 271, 39–51, https://doi.org/10.1016/j.palaeo.2008.09.010

De Zanche, V., Gianolla, P., Mietto, P., Siorpaes, C. 1993., Triassic sequence stratigraphy in the Dolomites (Italy). Memorie di Scienze Geologiche, 45, 1–27.

Dosztály, L., Kovács, S., Budai, T. 1989. Pécsely, Meggy hegy quarry. XXI European Micropalaeontological Colloquium, Guidebook.

Egli, M., Mirabella, A., Sartori, G. 2008. The role of climate and vegetation in weathering and clay mineral formation in late Quaternary soils of the Swiss and Italian Alps. Geomorphology, 102, 307-324, https://doi.org/10.1016/j.geomorph.2008.04.001

Fodor, L., Csontos, L., Bada, G., Győrfi, I., Benkovics, L., 1999. Tertiary tectonic evolution of the Pannonian Basin System and neighbouring orogens: a new synthesis of palaeostress data. In: Durand, B., Jolivet, L., Horváth, F., Séranne, M. (Eds.), The Mediterranean Basins: Tertiary Extension within the Alpine Orogen. Geological Society, London, Special Publications 156, 295–334, https://doi.org/10.1144/GSL.SP.1999.156.01.15

Franz, M., Kustatscher, E., Heunisch, C., Niegel, S., Röhling, H.-G., 2018. The Schilfsandstein and its flora – arguments for a humid mid-Carnian episode?. Journal of the Geological Society, *in press*, https://doi.org/10.1144/jgs2018-053

Franz, M., Nowak, K., Berner, U., Heunisch, C., Bandel, K., Röhling, H.-G., Wolfgamm, M., 2014. Eustatic and climatic control on the Upper Muschelkalk Sea (late Anisian/Ladinian) in the Central European Basin. Global and Planetary Change, 135, 1–27, https://doi.org/10.1016/j.gloplacha.2015.09.014

Furin, S., Preto, N., Rigo, M., Roghi, G., Gianolla, P., Crowley, J.L., Bowring, S.A., 2006. High-precision U-Pb zircon age from the Triassic of Italy: Implications for the Triassic time

scale and the Carnian origin of calcareous nannoplankton and dinosaurs. Geology, 34, 1009–1012, https://doi.org/10.1130/G22967A.1

Garzanti, E., 1985. The sandstone memory of the evolution of a Triassic volcanic arc in the Southern Alps, Italy. Sedimentology 32/3, 423–433, https://doi.org/ 10.1111/j.1365-3091.1985.tb00521.x

Garzanti, E., Pagni Frette, M., 1991. Il Carnico di Lierna (Como): Stratigrafia e paleogeografia. Rivista Italiana di Paleontologia e Stratigrafia 96/4, 407–426. (in Italian, with English Abstr.)

Garzanti, E., Padoan, M., Setti, M., Peruta, L., Najman, Y., Villa, I.M., 2013. Weathering geochemistry and Sr–Nd isotope fingerprinting of equatorial upper Nile and Congo muds. Geochemistry, Geophysics, Geosystems 14, 292–316, https://doi.org/10.1002/ggge.20060

Garzanti, E., Resentini, A., 2016. Provenance control on chemical indices of weathering (Taiwan river sands). Sedimentary Geology 336, 81–95, https://doi.org/10.1016/j.sedgeo.2015.06.013

Góczán, F., Csalagovics, I., Fügedi, P., Földvári, M., Detre, Cs., Haas, J., Kovács, S., Oravecz, J., Ravaszné Baranyai, L., Vető, I., 1979. A Zsámbék Zs–14 fúrás kútfúrási jegyzőkönyve és földtani naplója. Technical Report, Geological Institute of Hungary, data repository number: 1656/29 (in Hungarian)

Góczán, F., Haas, J., Lőrincz, H., Oravecz-Scheffer, A., 1983. Keszthelyi-hegység karni alapszelvény faciológiai és rétegtani értékelése. Magyar Állami Földtani Inézet Évi Jelentése 1981-ről, 263–293 (in Hungarian, with English Abstr.)

Góczán, F., Oravecz–Scheffer, A., 1996a. Tuvalian sequences of the Balaton Highland and the Zsámbék Basin, Part I: Litho-, bio- and chronostratigraphic subdivision. Acta Geol. Hung. 39, 1–31.

Góczán, F., Oravecz–Scheffer, A., 1996b. Tuvalian sequences of the Balaton Highland and the Zsámbék Basin, Part II: Characterization of sporomorph and foraminifer assemblages, biostratigraphic, palaeogeographic and geohistoric conclusions. Acta Geol. Hung. 39, 33–101.

Góczán, F., Oravecz–Scheffer, A., Csillag, G., 1991. Balatoncsicsó, Csukréti árok cordevolei és juli képződményeinek biosztratigráfiai jellemzése. Magyar Állami Földtani Inézet Évi Jelentése 1989-ről, pp. 241–323. (in Hungarian, with English Abstr.)

Haas, J., Budai, T., 1995. Upper Permian-Triassic facies zones in the Transdanubian Range. Riv. Ital. Paleontol. E Stratigr. Res. Paleontol. Stratigr 101, 249–266, https://doi.org/10.13130/2039-4942/8587

Haas, J., Budai, T., 1999. Triassic sequence stratigraphy of the Transdaubian Central Range (Hungary). Geologica Carpathica 50, 459–475.

Haas, J., Budai, T., 2014. A Dunántúli-középhegység felső-triász képződményeinek rétegtani- és fácieskérdései. Földtani Közlöny, 144, 125–142, (in Hungarian, with English Abstr.)

Haas, J., Budai, T., Csontos, L., Fodor, L., Konrád Gy., Koroknai, B., 2014. Explanatory notes for "Pre-Cenozoic geological map of Hungary" (1:500 000). Geological and Geophysical Institute of Hungary, Budapest.

Haas, J., Budai, T., Raucsik, B., 2012. Climatic controls on sedimentary environments in the Triassic of the Transdanubian Range (Western Hungary). Palaeogeography, Palaeoclimatology, Palaeoecology, 353–355, 31–44, https://doi.10.1016/j.palaeo.2012.06.031

Haas, J., Kovács, S., 2012. Pelso Composite Unit- Geology and History of Evolution of the ALCAPA Mega-Unit. In: Haas, J. (Ed.), Geology of Hungary, Springer Berlin-Heidelberg, 21-81.

Haas, J., Kovács, S., Krystyn, L., Lein, R., 1995. Significance of Late Permian–Triassic facies zones in terrane reconstructions in the Alpine–North Pannonian domain. Tectonophysics 242, 19–40, https://doi.org/10.1016/0040-1951(94)00157-5

Haas, J., Oravecz, J., Góczán, F., 1981. Jelentés a Zsámbék, Zs–14. sz. alapszelvény fúrás vizsgálatáról. Technical Report, 1656/29, Geological Institute of Hungary (in Hungarian)

Harper, D.A.T., 1999. Numerical palaeobiology, John Wiley & Sons, New York

Hornung, T., Brandner, R., 2005. Biochronostratigraphy of the Reingraben Turnover (Hallstatt Facies Belt): Local black shale events controlled by regional tectonics, climatic change and plate tectonics. Facies 51, 460–479. https://doi.org/10.1007/s10347-005-0061-x

Hornung, T., Brandner, R., Krystyn, L., Joachimsky, M.M., Keim, L., 2007a. Multistratigraphic constraints on the NW Tethyan "Carnian Crisis". N. M.Mus.Nat. Hist. Sci. Bull. 4, 9–67.

Hornung, T., Krystyn, L., Brandner, R., 2007b. A Tethys-wide mid-Carnian (Upper Triassic) carbonate productivity decline: evidence for the Alpine Reingraben Event from Spiti (Indian Himalaya). J. Asian Earth Sci. 30, 285–302. https://dx.doi.org/10.1016/j.jseaes.2006.10.001.

Jelen, B., Kušej, J., 1982. Quantitative palynological analysis of Julian clastic rocks from the lead-zinc deposit of Mežica. Geologija Geological Transactions and Reports 25, 213–227.

Kavary, E., 1966. A palynological study of the subdivision of the Cardita Shales (Upper Triassic) of Bleiberg, Austria. Verhandlungen der Geologische Bundesanstalt 1–2, 178–189.

Kavary, E., 1972. Significant Upper Triassic microspores from Bleiberg, (Austria). Jahrbuch der Geologischen Bundesanstalt 19, 87–105.

Kázmér M. & Kovács S. 1985. Permian-Paleogene paleogeography along the eastern part of the Insubric-Periadriatic lineament system: Evidence for continental escape of the Bakony-Drauzug unit. Acta Geologica Hungarica 28, 71–84.

Keim, L., Spötl, C. & Brandner, R., 2006. The aftermath of the Carnian carbonate platform demise: a basinal perspective (Dolomites, Southern Alps). Sedimentology 53, 361–386, https://doi.10.1111/j.1365-3091.2006.00768.x

Kovács, S., Krystyn, L., Szabó, S., Dosztály, L., Budai, T., 1991. The Ladinian/Carnian boundary in the Balaton Upland, Hungary. Symp. Trias. Strat., Lausanne, Abstracts, 39.

Kristan-Tollmann, E. Haas, J., Kovács, S., 1991. Karnische Ostracoden und Conodonten der Bohrung Zsámbék–14 im Transdanubischen Mittelgebirge (Ungarn). In: Lobitzer, H., Császár, G. (Eds.) Jubiläumsschrift 20 Jahre Geologische Zusammenarbeit Österreich–Ungarn I, 193–220.

Kustatscher, E., Heunisch, C., Van Konijnenburg-Van Cittert, J.H.A., 2012. Taphonomical implications of the Ladinian megaflora ans palynoflora of Thale (Germany). Palaios 27, 753–764, https://doi.10.2110/palo.2011.p11-090r

Kürschner, W.M., Herngreen, G.F.W., 2010. Triassic palynology of central and northwestern Europe: a review of palynofloral diversity patterns and biostratigraphic subdivisions. Geological Society of London Special Publication 334, 263–283, https://doi:10.1144/SP334.11

Langenheim, J.H. 2013. Plant resins: Chemistry, Evolution, Ecology, Ethnobotany. Timber Press, Portland, Cambridge.

Lindström, S., Erlström, M., Piasecki, S., Nielsen, L.H., Mathiesen, A., 2017. Palynology and terrestrial ecosystem change of the Middle Triassic to lowermost Jurassic succession of the eastern Danish Basin. Review of Palaeobotany and Palynology 244, 65–95, https://doi.org/10.1016/j. revpalbo.2017.04.007

Lukeneder, S., Lukeneder, A., Harzhauser, M., İslamoğlu, Y., Krystyn, L. & Lein, R. 2012. A delayed carbonate factory breakdown during the Tethyan-wide Carnian Pluvial Episode along the Cimmerian terranes (Taurus, Turkey). Facies 58, 279–296, https://doi.10.1007/s10347-011-0279-8

Márton, E., Fodor, L., 2003. Tertiary paleomagnetic results and structural analysis from the Transdanubian Range (Hungary): rotational disintegration of the Alcapa unit. Tectonophysics 363, 201–224, https://doi.org/10.1016/S0040-1951(02)00672-8

McArthur, A.D., Jolley, D.W., Hartley, A.J., Archer, S.G., Lawrence, H.M., 2016. Palaeoecology of syn-rift topography: A Late Jurassic footwall island on the Josephine Ridge, Central Graben, North Sea. Palaeogeography, Palaeoclimatology, Palaeoecology 459, 63–75, https://doi.org/10.1016/j.palaeo.2016.06.033

Miller, C.S., Peterse, F., da Silva, A-C., Baranyi, V., Reichart, G.J., Kürschner, W.M., 2017. Astronomical age constraints and extinction mechanisms of the Late Triassic Carnian crisis. Scientific Reports, 7:2557, https://doi.10.1038/s41598-017-02817-7

Mueller, S., Hounslow, M.W., Kürschner, W.M. 2016a. Integrated stratigraphy and palaeoclimate history of the Carnian Pluvial Event in the Boreal realm; new data from the

Upper Triassic Kapp Toscana Group in central Spitsbergen (Norway). Journal of the Geological Society 173, 186–202, https://doi.10.1144/jgs2015-028

Mueller, S., Krystyn, L., Kürschner, W.M., 2016b. Climate variability during the Carnian Pluvial Phase — A quantitative palynological study of the Carnian sedimentary succession at Lunz am See, Northern Calcareous Alps, Austria. Palaeogeography, Palaeoclimatology, Palaeoecology 441, 198–211, http://dx.doi.org/10.1016/j.palaeo.2015.06.008

Nakada, R., Ogawa, K., Suzuki, N., Takahashi, S., Takahashi, Y., 2014. Late Triassic compositional changes of aeolian dusts in the pelagic Panthalassa: response to the continental climatic change. Palaeogeography, Palaeoclimatology, Palaeoecology 393, 61–75, https://doi.org/10.1016/j.palaeo.2013.10.014

Ogg, J.G., 2015. The mysterious Mid-Carnian "Wet Intermezzo" global event. Journal of Earth Science 26, 181–191, https://doi.10.1007/s12583-015-0527-x

Planderová, E., 1980. Palynomorphs from Lunz Beds and from black clayey shales in basement of Vienna Basin (borehole LNV-7). Geologica Carpathica 31, 267–294.

Pott, C., Krings, M., Kerp, H. 2008. The Carnian (Late Triassic) flora from Lunz in Lower Austria: paleoecological considerations. Palaeoworld 17, 172–182, https://doi.org/10.1016/j.palwor.2008.03.001

Preto, N., Kustatscher, E., Wignall, P.B., 2010. Triassic climates — State of the art and perspectives. Palaeogeography, Palaeoclimatology, Palaeoecology 290, 1–10, https://doi.org/10.1016/j.palaeo.2010.03.015

Raucsik, B., Varga, A., 2008. Climato-environmental controls on clay mineralogy of the Hettangian–Bajocian successions of the Mecsek Mountains, Hungary: an evidence for extreme continental weathering during the early Toarcian oceanic anoxic event. Palaeogeography Palaeoclimatology Palaeoecology 265, 1–13, https://doi.org/10.1016/j.palaeo.2008.02.004

Raucsik, B., Horváth, H., Varga, A. 2005. A Sándorhegyi Formáció szervetlen geokémiai vizsgálatának eredményei (Pécselyi Tagozat, Nosztori-völgy). Földtani Közlöny, 135, 543–569, (in Hungarian, with English Abstr.)

Rigo, M., Joachimski, M.M., 2010. Palaeoecology of Late Triassic conodonts: constraints from oxygen isotopes in biogenic apatite. Acta Palaeontol. Pol. 55, 471–478. https://dx.doi.org/10.4202/app.2009.0100

Rigo, M., Preto, N., Roghi, G., Tateo, F., Mietto, P., 2007. A rise in the Carbonate Compensation Depth of western Tethys in the Carnian: deep-water evidence for the Carnian Pluvial Event. Palaeogeography, Palaeoclimatology, Palaeoecology 246, 188–205, https://doi.org/10.1016/j.palaeo.2006.09.013

Roghi, G. 2004. Palynological investigations in the Carnian of the Cave del Predil area (Julian Alps, NE Italy). Rev. Palaeobot. Palynol 132, 1–35, https://doi.org/10.1016/j.revpalbo.2004.03.001

Roghi, G., Gianolla, P., Minarelli, L., Pilati, C., Preto, N., 2010. Palynological correlation of Carnian humid pulses throughout western Tethys. Palaeogeography, Palaeoclimatology, Palaeoecology 290, 89–106, https://doi.org/10.1016/j.palaeo.2009.11.006

Roghi, G., Ragazzi, E., Gianolla, P., 2006. Triassic amber of the Southern Alps. PALAIOS 21, 143–154, https://doi.org/10.2110/palo.2005.p05-68

Rostási, Á. 2011. Palaeoenvironmental reconstruction of the Carnian (Late Triassic) of the Gerencse and Bakony Basins, based on mineralogy and petrology. Ph.D. Thesis, University of Pannonia, Veszprém (in Hungarian, with English Abstr.).

Rostási, Á., Raucsik, B., Varga, A., 2011. Palaeoenvironmental controls on the clay mineralogy of Carnian sections from the Transdanubian Range (Hungary). Palaeogeography, Palaeoclimatology, Palaeoecology 300, 101–112, https://doi.org/10.1016/j.palaeo.2010.12.013

Ruffell, A., McKinley, J.M., Worden, R.H., 2002. Comparison of clay mineral stratigraphy to other proxy palaeoclimate indicators in the Mesozoic of NW Europe. Philos. Trans. A Math. Phys. Eng. Sci. 360, 675–693, https://doi.10.1098/rsta.2001.0961

Ruffell, A., Simms, M. J., Wignall, P.B., 2016. The Carnian Humid Episode of the late Triassic: a review. Geological Magazine 153, 271–284, https://doi.10.1017/S0016756815000424

Schlager, W., Schöllnberger, W., 1974. Das Prinzip stratigraphischer Wenden in der Schichtenfolge der Nordlichen Kalkalpen. Mitteilungen der Geologischen Gesellschaft Wien, 66/67, 165–93 (in German)

Schneider, S., Hornung, J., Hinderer, M., Garzanti, E., 2016. Petrography and geochemistry of modern river sediments in an equatorial environment (Rwenzori Mountains and Albertine rift, Uganda) - Implications for weathering and provenance. Sedimentary Geology 336, 106–119, https://doi.org/10.1016/j.sedgeo.2016.02.006

Simms, M.J., Ruffell, A.H., 1989. Synchroneity of climatic change and extinctions in the Late Triassic. Geology 17, 265–268, https://doi.10.1130/0091-7613(1989)017<0265:SOCCAE>2.3.CO;2

Simms, M.J., Ruffell, A.H., 1990. Climatic and biotic change in the Late Triassic. Journal of the Geological Society, London 147, 321–327, https://doi.org/10.1144/gsjgs.147.2.0321

Simms, M.J., Ruffel, A.H., Johnson, L.A., 1995. Biotic and climatic changes in the Carnian (Triassic) of Europe and adjacent areas. In: Fraser, N.C., Sues, H.-D. (Eds.), In the Shadow of the Dinosaurs: Early Mesozoic Tetrapods. Cambridge University Press, pp. 352–365.

Sladen, C.P., Batten, D.J., 1984. Source-area environments of Late Jurassic and Early Cretaceous sediments in south-east England. Proceedings of the Geologists' Association 95, 2, 149–163, https://doi.org/10.1016/S0016-7878(84)80002-4

Slater, S.M., McKie, T., Vieira, M., Wellman, C.H., Vajda, V., 2017. Episodic river flooding events revealed by palynological assemblages in Jurassic deposits of the Brent Group, North Sea. Palaeogeography, Palaeoclimatology, Palaeoecology 485, 389–400, https://doi.org/10.1016/j.palaeo.2017.06.028

Sun, Y.D., Wignall, P.B., Joachimski, M.M., Bond, D.P.G., Grasby, S.E., Lai, X.L., Wang, L.N., Zhang, Z.T., Sun, S., 2016. Climate warming, euxinia and carbon isotope perturbations during the Carnian (Triassic) Crisis in South China. Earth and Planetary Science Letters 444, 88–100, https://doi.org/10.1016/j.epsl.2016.03.037

Trotter, J.A., Williams, I.S., Nicora, A., Mazza, M., Rigo, M., 2015. Long-term cycles of Triassic climate change: A new δ18O record from conodont apatite. Earth Planetary Science Letters 415, 165–174, https://doi.org/10.1016/j.epsl.2015.01.038

Vakhrameev, V.A., 1991. Jurassic and Cretaceous floras and climates of the Earth. Cambridge University Press, Cambridge

Van der Eem, J.G.L.A. 1983. Aspects of middle and late triassic palynology. 6. Palynological investigations in the Ladinian and lower Karnian of the Western Dolomites, Italy. Rev. Palaeobot. Palynol 39, 189–300, https://doi.org/10.1016/0034-6667(83)90016-7

Viczián, I., 1995. Clay minerals in Mesozoic and Paleogene sedimentary rocks of Hungary. Roman. J. Mineral. 77, 35–44.

Visscher, H., Van Houte, M., Brugman, W.A. & Poort, R.J. 1994. Rejection of a Carnian (Late Triassic) "pluvial event" in Europe. Rev. Palaeobot. Palynol 83, 217–226, https://doi.org/10.1016/0034-6667(94)90070-1

Visscher, H., Van der Zwan, C.J., 1981. Palynology of the circum-Mediterranean Triassic phytogeographical and palaeoclimatological implications. Geologische Rundschau 70, 625–636.

Whiteside, J.H., Lindström, S., Irmis, R.B., Glasspool, I.J., Schaller, M.F., Dunlavey, M., Nesbitt, S.J., Smith, N.D., Turner, A.H., 2015. Extreme ecosystem instability suppressed tropical dinosaur dominance for 30 million years. Proceedings of the National Academy of Sciences 112, 7909–7913, https://doi.10.1073/pnas.1505252112

Zhang, L., Wang, J., Bai, Z., Lv, C., 2015. Effects of vegetation on runoff and soil erosion on reclaimed land in an opencast coal-mine dump in a loess area. Catena 128, 44–53. https://doi.org/10.1016/j.catena.2015.01.016

Figure captions

Fig. 1. Geological and palaeogeographical setting of the Transdanubian Range. A. The geological framework and the major tectonic units of the Carpathian–Pannonian Basin (after Csontos & Vörös 2004). The box indicates the area shown in 1B. B. Generalized geological map of the Transdanubian Range modified after Haas & Kovács (2012) and Rostási et al (2011) showing the locality of the three studied boreholes. C. Palaeogeographical setting of the Transdanubian Range in the western Neotethys during the Late Triassic. Modified after Haas et al. (1990, 2016). D. Schematic palaeogeographical model for the depositional area of the Veszprém Marl Formation in the late Julian. Modified from Haas & Budai (1995). [**color**, **2 columns fitting]**

Fig. 2. Lithostratigraphical subdivision of the Upper Triassic formations in the Transdanubian Range, modified after Haas & Budai (2014). [**color**, **1.5 columns fitting]**

Fig. 3. Schematic lithological logs and the positions of the investigated samples in the three boreholes showing the stratigraphic framework. Abbreviations: Fm Formation, SF Sándorhegy Formation, Jul. Julian, Tuv. Tuvalian. Modified from Rostási (2011), Rostási et al. (2011). Stratigraphical information from Góczán & Oravecz-Scheffer (1996a, b) and Dal Corso et al. (2015, 2018). **[color, 2 column fitting]**

Fig. 4. Relative abundances of terrestrial palynomorphs and palynomorph assemblages through the Veszprém Marl Formation within the Met–1 and V-1 boreholes. The grey area of the curves is exaggeration (3X) of the abundances plotted in black. **[greyscale, 2 columns fitting]**

Fig. 5 Relative abundances of terrestrial and aquatic palynomorphs in the uppermost part of the Csákberény Formation within the Zs–14 borehole. **[2 columns fitting]**

Fig. 6. PCA ordination diagram of the pollen and spore taxa in the three studied boreholes. **[color, 1.5 columns fitting]**

Fig. 7. The trends in the α-indices (α^{Al}_{Ba}, α^{Al}_{K}, α^{Al}_{Na}) in the Met-1, V-1 and Zs-14 sections. **[black and white, 2 columns fitting]**

Fig. 8. Relative abundance of the various sporomorph ecogroups, ratio of hygrophytic to xerophytic palynomorphs, First and second principal components and their comparison to the variations in the kaolinite content in the Met–1 and V–1. Bulk organic carbon isotope values of the Met-1 is from Dal Corso et al. (2018). Abbreviations: NLM = Nosztor Limestone, SDM = Sédvölgy Dolomite . **[color, 2 columns fitting]**

Fig. 9. Relative abundance of the various sporomorph ecogroups, ratio of hygrophytic to xerophytic palynomorphs, first and second principal components and their comparison to the variations in the kaolinite content in the Zs-14 section. Abbreviations: Tuv. = Tuvalian, CsF = Csákberény Formation **[2 columns fitting]**

Fig. 10. Chemostratigraphic correlation of the carbon-isotope records from the marine marginal successions of the Western Tethys realm and climate evolution of the TR during the Carnian Pluvial Episode (Dal Corso et al. 2012, 2015, 2018). Three, possibly four negative carbon isotope excursions (NCIEs) punctuated the CPE. In the Western Tethys realm these excursions are tentatively linked to the increase of clastic input into marine sedimentary

basins and discrete humid climatic episodes. The grey bars correlate the four negative carbon-isotope excursions (NCIEs). The correlation of the NCIE-3 from the Dolomites and Julian Alps to the recorded NCIE at the top of the Csákberény Formation proposed by Dal Corso et al. (2018) is not straightforward. The age of the Csákberény Formation in the Zs-14 is not well constrained biostratigraphically as sporomorphs from the Zs-14 give only a Carnian age but do not allow a more precise age assignment. Climate proxies (hygrophytic/xerophytic sporomorph ratios and kaolinite proportions) from the TR in Hungary suggest a humid period for the early Julian 2 (Mencshely Marl) and probably the late Julian 2 (Csicsó Marl). The climate returned to arid conditions in the Tuvalian. Abbreviations and references: Dolomites (Dal Corso et al. 2012, 2015, 2018). Julian Alps (Dal Corso et al. 2012, 2015, 2018), Transdanubian Range (Rostási et al. 2011; Dal Corso et al. 2018), VMF= Veszprém Formation, CsMM=Csicsó Marl. Lunz (Dal Corso et al. 2015; Mueller et al. 2016b), R.graben=Reingraben Formation, Göst.=Göstling Member. **[colour, full spread]**

Highlights

- New quantitative palynological data from three CPE sections from the western Tethys (from the Transdanubian Range, western Hungary)
- Palaeoclimatic trends inferred from multivariate statistical analysis of palynomorphs and geochemical weathering proxies
- Shift to hygrophyte vegetation, wetter climate and enhanced continental hydrolysis in the early Julian 2 and return to xerophyte assemblages and drier climate in the Tuvalian
- Weathering proxies suggest enhanced continental hydrolyses only in the early stages of the CPE in the early Julian 2
- Correlation of the clastic pulses within the western Tethys based on the palynological assemblages

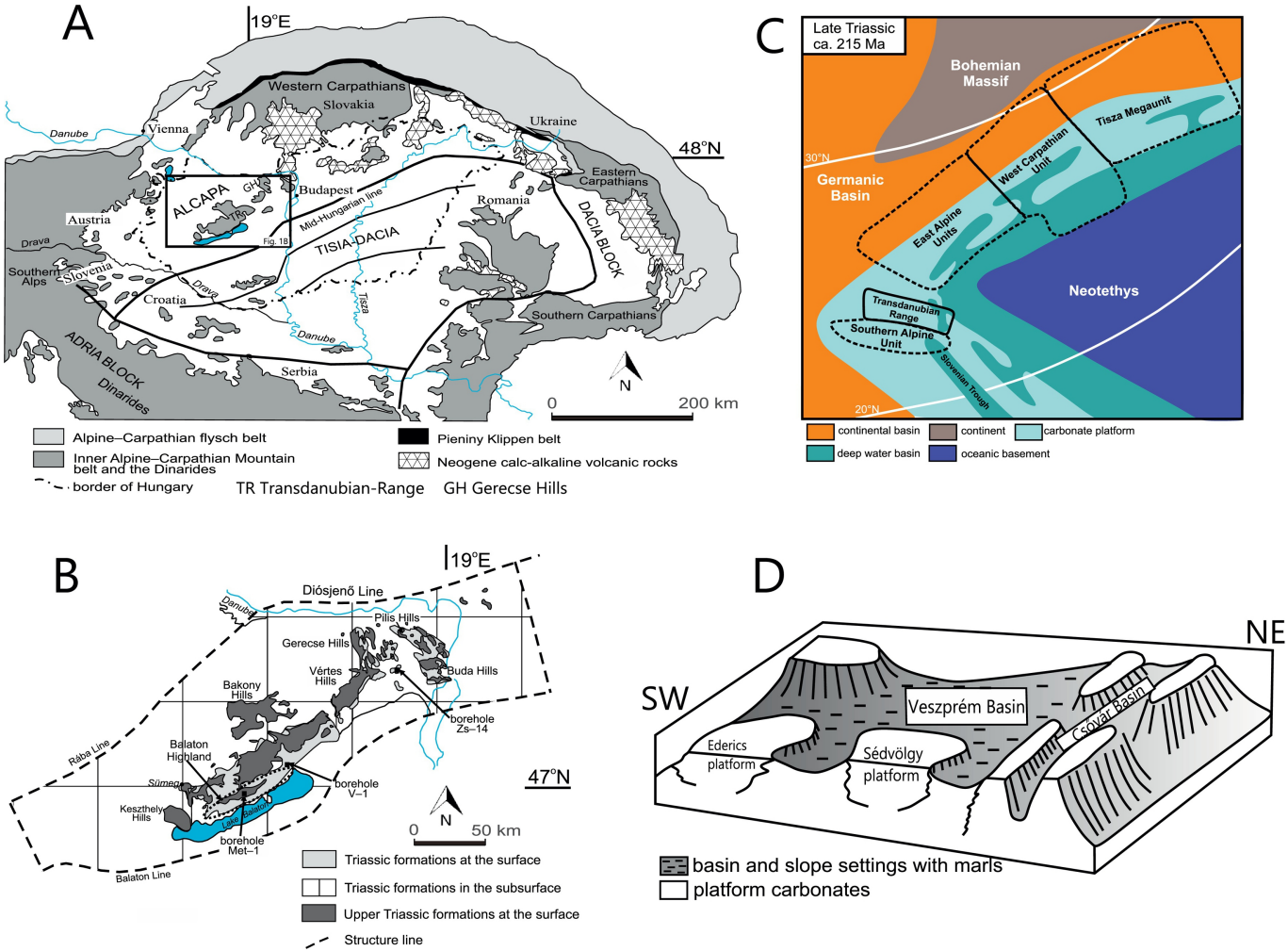
A
19°E
Western Carpathians
Slovakia
Ukraine
Vienna
Danube
48°N
Budapest
ALCAPA
GH
TR
Fig. 1B
Mid-Hungarian line
Romania
Eastern Carpathians
DACIA BLOCK
Austria
Drava
TISIA-DACIA
Southern Alps
Slovenia
Croatia
Tisza
Southern Carpathians
ADRIA BLOCK
Dinarides
Serbia
N
0
200 km
Alpine–Carpathian flysch belt
Inner Alpine–Carpathian Mountain belt and the Dinarides
border of Hungary
Pieniny Klippen belt
Neogene calc-alkaline volcanic rocks
TR Transdanubian-Range
GH Gerecse Hills
C
Late Triassic
ca. 215 Ma
Bohemian Massif
Tisza Megaunit
30°N
Germanic Basin
West Carpathian Unit
East Alpine Units
Neotethys
Transdanubian Range
Southern Alpine Unit
Slovenian Trough
20°N
continental basin
continent
carbonate platform
deep water basin
oceanic basement
B
19°E
Diósjenő Line
Danube
Pilis Hills
Gerecse Hills
Vértes Hills
Buda Hills
Bakony Hills
borehole Zs–14
Balaton Highland
Rába Line
Sümeg
borehole V–1
47°N
Keszthely Hills
Lake Balaton
borehole Met–1
0
50 km
Balaton Line
Triassic formations at the surface
Triassic formations in the subsurface
Upper Triassic formations at the surface
Structure line
D
SW
NE
Veszprém Basin
Csővár Basin
Ederics platform
Sédvölgy platform
basin and slope settings with marls
platform carbonates

Figure 1

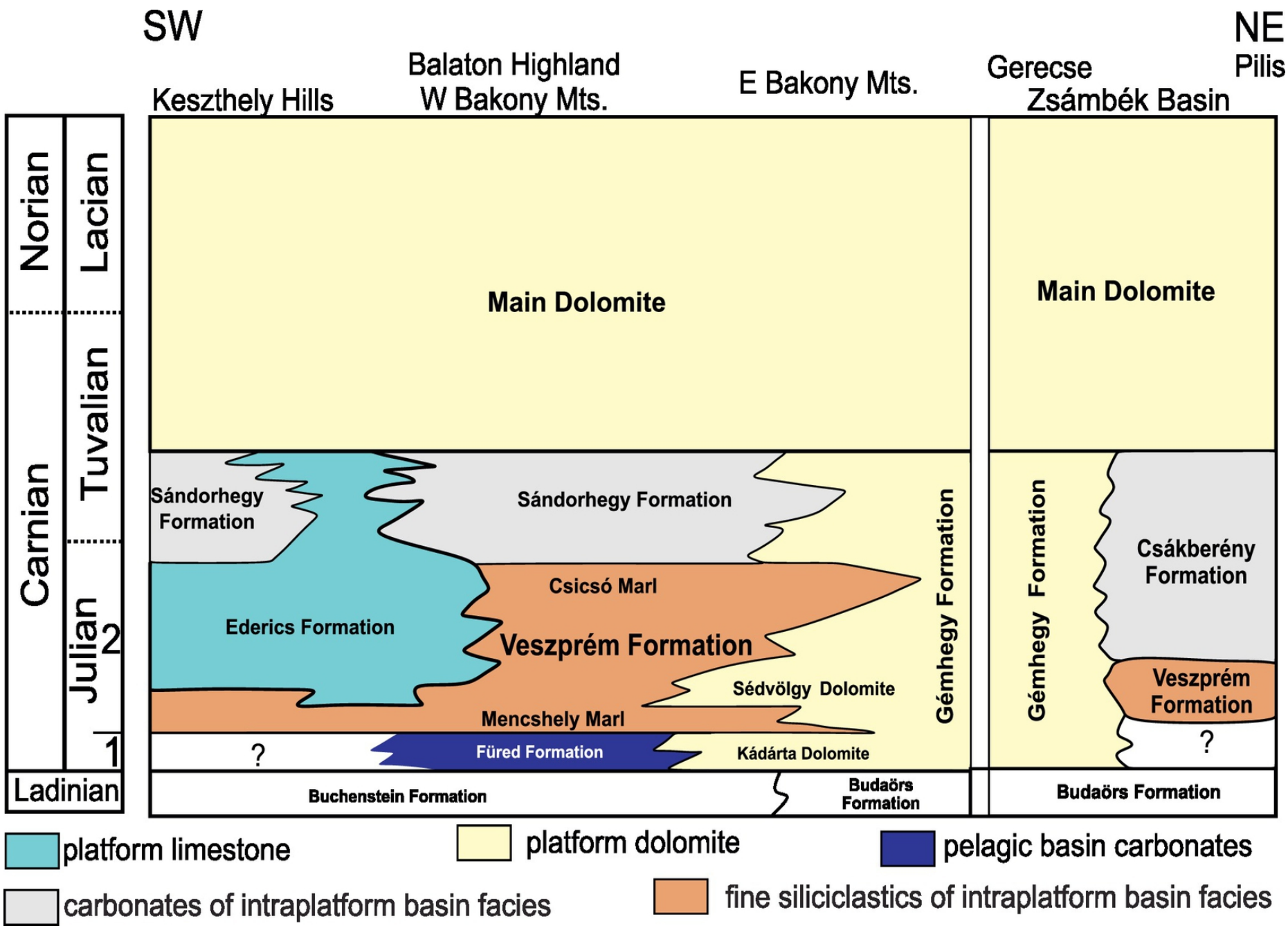
SW
NE
Keszthely Hills
Balaton Highland
W Bakony Mts.
E Bakony Mts.
Gerecse
Zsámbék Basin
Pilis
Norian
Lacian
Tuvalian
Carnian
Julian 2
Julian 1
Ladinian
Main Dolomite
Main Dolomite
Sándorhegy Formation
Sándorhegy Formation
Csicsó Marl
Ederics Formation
Veszprém Formation
Sédvölgy Dolomite
Mencshely Marl
Füred Formation
Kádárta Dolomite
Gémhegy Formation
Gémhegy Formation
Csákberény Formation
Veszprém Formation
?
?
Buchenstein Formation
Budaörs Formation
Budaörs Formation
platform limestone
platform dolomite
pelagic basin carbonates
carbonates of intraplatform basin facies
fine siliciclastics of intraplatform basin facies

Figure 2

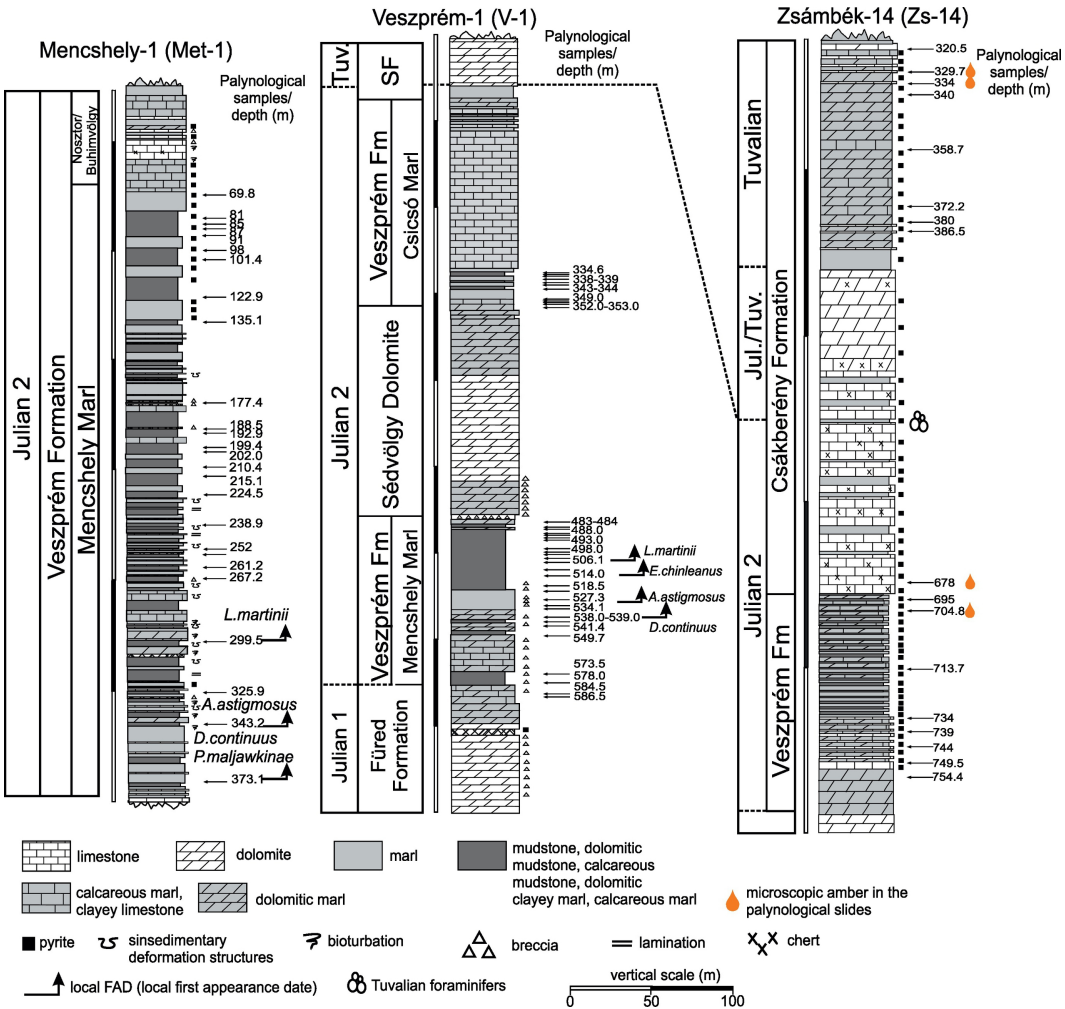
Mencshely-1 (Met-1)
Veszprém-1 (V-1)
Zsámbék-14 (Zs-14)
Palynological samples/ depth (m)
Julian 2
Veszprém Formation
Mencshely Marl
Noszlop/ Buhimvölgy
Tuv.
SF
Veszprém Fm
Csicsó Marl
Sédvölgy Dolomite
Julian 1
Füred Formation
Tuvalian
Jul./Tuv.
Csákberény Formation
69.8
81
85
87
91
98
101.4
122.9
135.1
177.4
188.5
192.9
199.4
202.0
210.4
215.1
224.5
238.9
252
261.2
267.2
L.martinii
299.5
325.9
A.astigmosus
343.2
D.continuus
P.maljawkinae
373.1
334.6
338-339
343-344
349.0
352.0-353.0
483-484
488.0
493.0
498.0
506.1
514.0
518.5
527.3
534.1
538.0-539.0
541.4
549.7
L.martinii
E.chinleanus
A.astigmosus
D.continuus
573.5
578.0
584.5
586.5
320.5
329.7
334
340
358.7
372.2
380
386.5
678
695
704.8
713.7
734
739
744
749.5
754.4
limestone
dolomite
marl
mudstone, dolomitic
mudstone, calcareous
mudstone, dolomitic
clayey marl, calcareous marl
calcareous marl, clayey limestone
dolomitic marl
microscopic amber in the palynological slides
pyrite
sinsedimentary deformation structures
bioturbation
breccia
lamination
chert
local FAD (local first appearance date)
Tuvalian foraminifers
vertical scale (m)
0
50
100

Figure 3

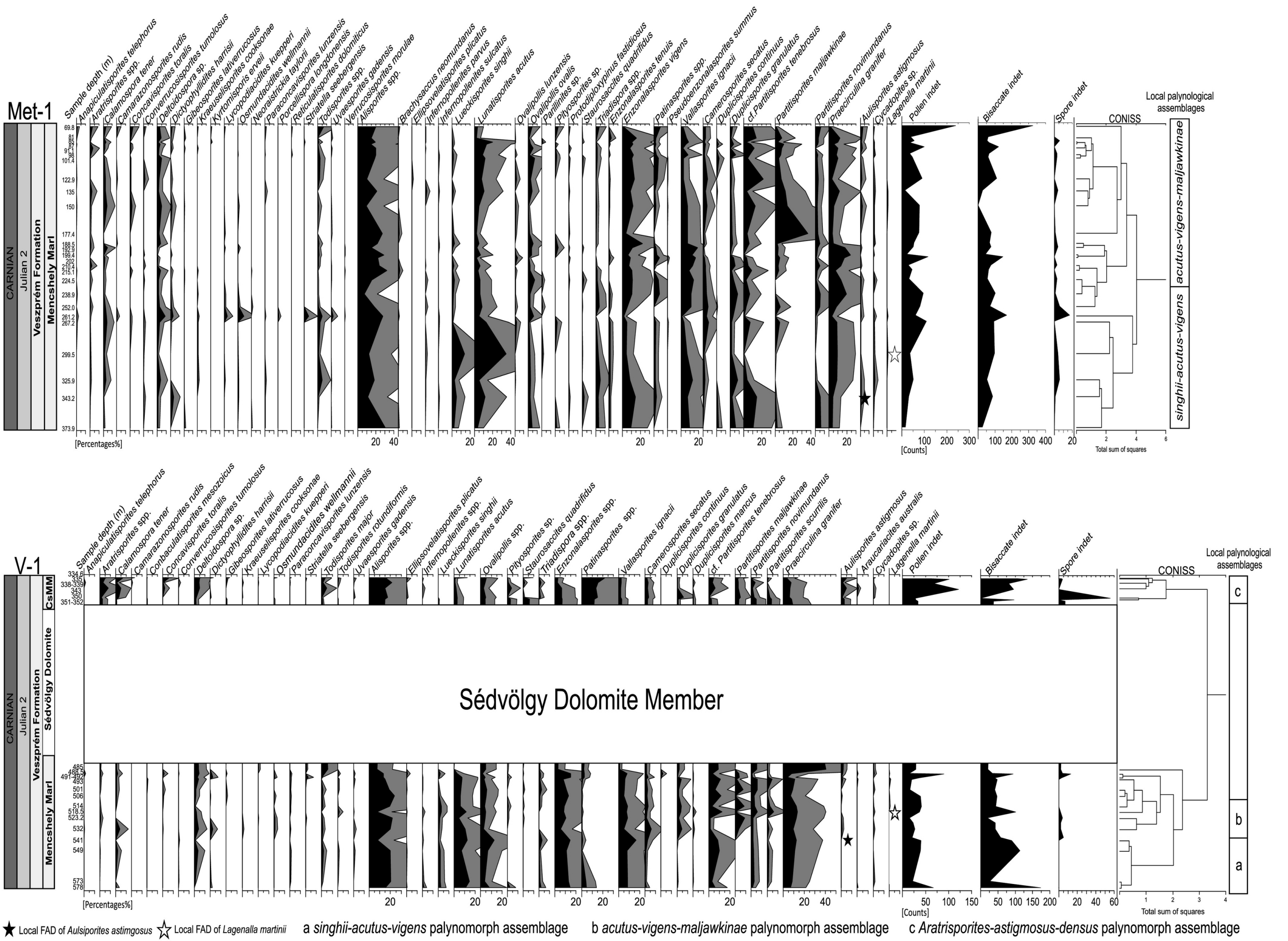

Met-1
Sample depth (m)
Anapiculatisporites telephorus
Aratrisporites spp.
Calamospora tener
Camarazonosporites rudis
Concavisporites toralis
Converrucosisporites tumulosus
Deltoidospora sp.
Dictyophyllidites harrisii
Gibeosporites lativerrucosus
Kraeuselisporites cooksonae
Kyrtomisporis ervei
Lycopodiacidites kuepperi
Osmundacidites wellmannii
Neoraistrickia taylorii
Paraconcavisporites lunzensis
Porcellispora longdonensis
Reticulatisporites dolomiticus
Striatella seebergensis
Todisporites spp.
Uvaesporites gadensis
Verrucosisporites morulae
Alisporites spp.
Brachysaccus neomundanus
Ellipsovelatisporites plicatus
Infernopollenites parvus
Infernopollenites sulcatus
Lueckisporites singhii
Lunatisporites acutus
Ovalipollis lunzensis
Ovalipollis ovalis
Parillinites sp.
Pityosporites sp.
Protodiploxypinus fastidiosus
Staurosaccites quadrifidus
Triadispora spp.
Enzonalasporites tenuis
Enzonalasporites vigens
Patinasporites spp.
Pseudoenzonalasporites summus
Vallasporites ignacii
Camerosporites secatus
Duplicisporites continuus
Duplicisporites granulatus
cf. Partitisporites tenebrosus
Partitisporites maljawkinae
Partitisporites novimundanus
Praecirculina granifer
Aulisporites astigmosus
Cycadopites sp.
Lagenella martinii
Pollen indet
Bisaccate indet
Spore indet
CONISS
Local palynological assemblages
CARNIAN
Julian 2
Veszprém Formation
Mencshely Marl
acutus-vigens-maljawkinae
singhii-acutus-vigens
[Percentages%]
[Counts]
Total sum of squares
V-1
Araucariacites australis
Conbaculatisporites mesozoicus
Todisporites major
Todisporites rotundiformis
Infernopollenites spp.
Enzonalasporites spp.
Duplicisporites mancus
Partitisporites scurrilis
CsMM
Sédvölgy Dolomite
Sédvölgy Dolomite Member
a
b
c
Local FAD of Aulsiporites astimgosus
Local FAD of Lagenalla martinii
a singhii-acutus-vigens palynomorph assemblage
b acutus-vigens-maljawkinae palynomorph assemblage
c Aratrisporites-astigmosus-densus palynomorph assemblage

Figure 4

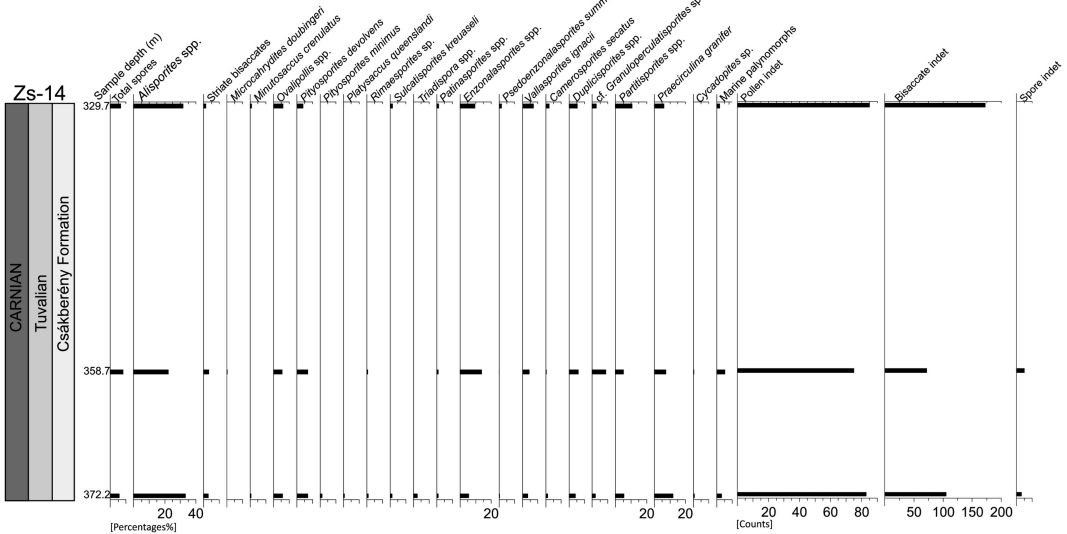
Zs-14
CARNIAN
Tuvalian
Csákberény Formation
Sample depth (m)
Total spores
Alisporites spp.
Striate bisaccates
Microcachrydites doubingeri
Minutosaccus crenulatus
Ovalipollis spp.
Pityosporites devolvens
Pityosporites minimus
Platysaccus queenslandi
Rimaesporites sp.
Sulcatisporites kreuselli
Triadispora spp.
Patinasporites spp.
Enzonalasporites spp.
Pseudenzonalasporites summus
Vallasporites ignacii
Camerosporites secatus
Duplicisporites spp.
cf. Granuloperculatisporites sp.
Partitisporites spp.
Praecirculina granifer
Cycadopites sp.
Marine palynomorphs
Pollen indet
Bisaccate indet
Spore indet
329.7
358.7
372.2
20
40
[Percentages%]
20
20
20
40
60
80
[Counts]
50
100
150
200

Figure 5

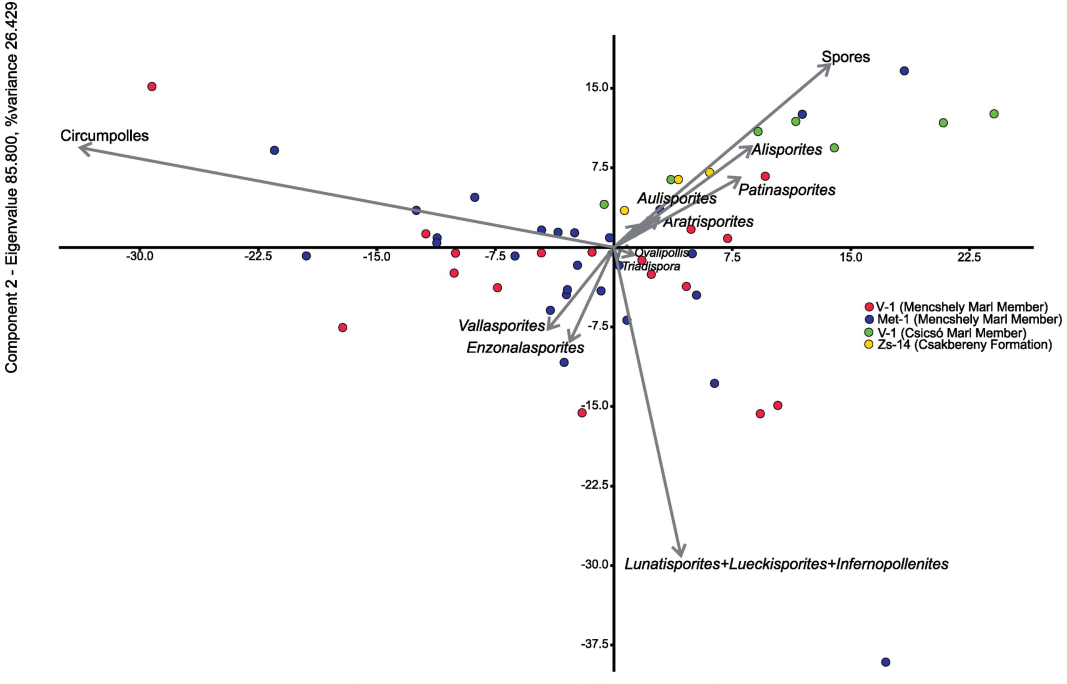
Component 2 - Eigenvalue 85.800, %variance 26.429
Component 1 - Eigenvalue 111.133, % variance 34.232
Spores
Circumpolles
Alisporites
Patinasporites
Aulisporites
Aratrisporites
Ovalipollis
Triadispora
Vallasporites
Enzonalasporites
Lunatisporites+Lueckisporites+Infernopollenites
V-1 (Mencshely Marl Member)
Met-1 (Mencshely Marl Member)
V-1 (Csicsó Marl Member)
Zs-14 (Csakbereny Formation)
15.0
7.5
-7.5
-15.0
-22.5
-30.0
-37.5
-30.0
-22.5
-15.0
-7.5
7.5
15.0
22.5

Figure 6

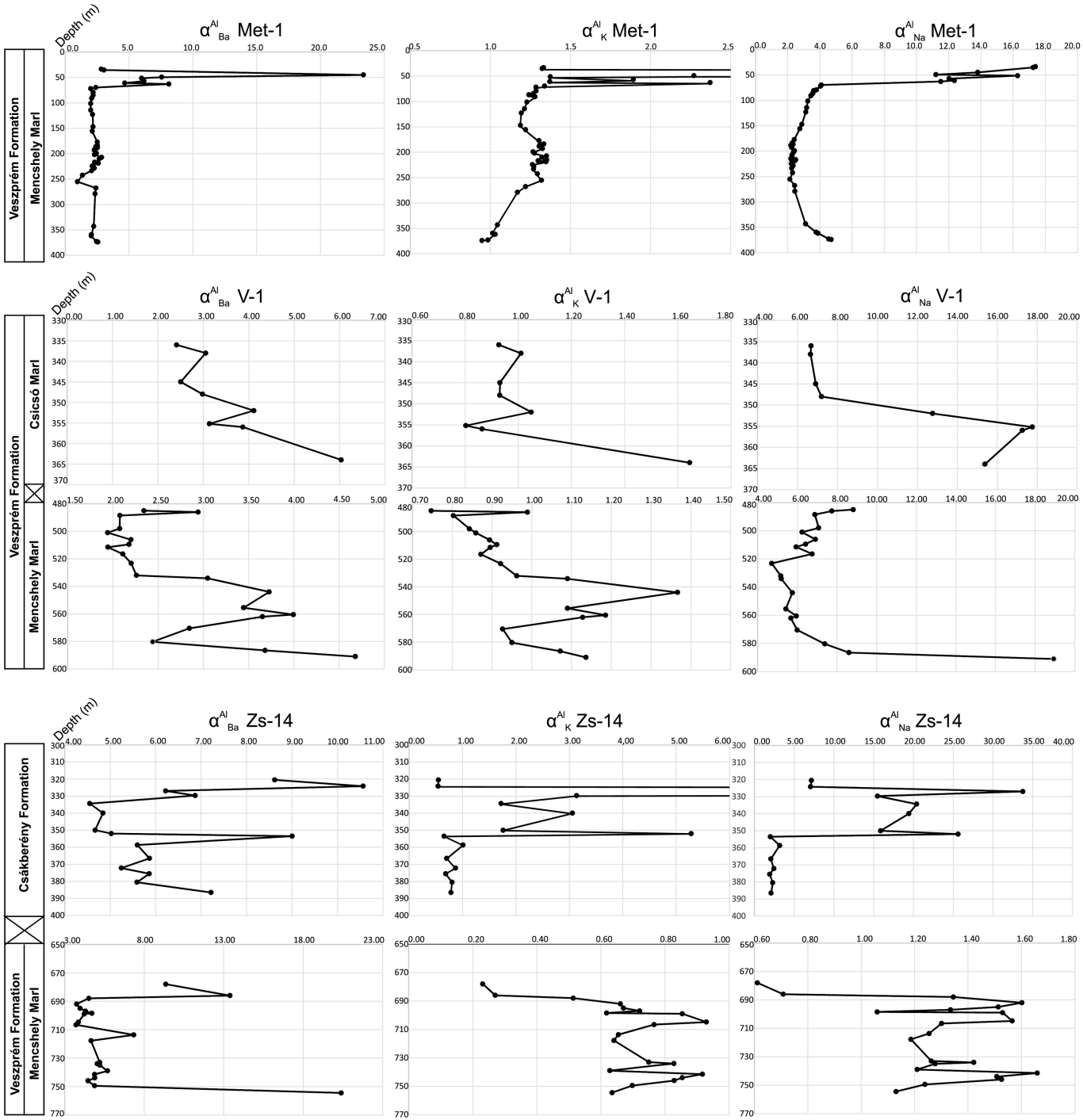
Depth (m)
α^{Al}_{Ba} Met-1
α^{Al}_{K} Met-1
α^{Al}_{Na} Met-1
α^{Al}_{Ba} V-1
α^{Al}_{K} V-1
α^{Al}_{Na} V-1
α^{Al}_{Ba} Zs-14
α^{Al}_{K} Zs-14
α^{Al}_{Na} Zs-14
Veszprém Formation
Mencshely Marl
Csicsó Marl
Csákberény Formation

Figure 7

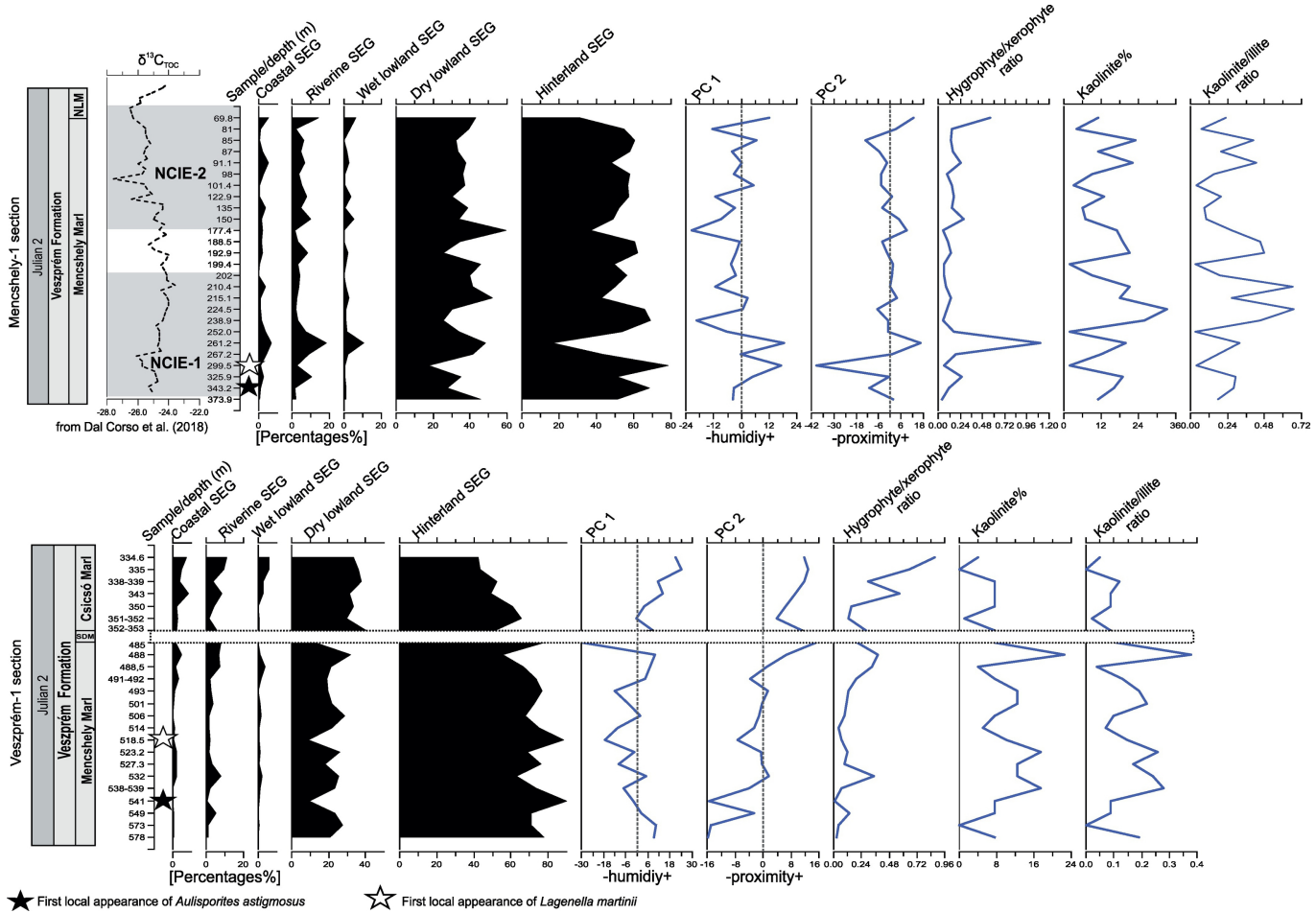
Mencshely-1 section
Julian 2
Veszprém Formation
Mencshely Marl
NLM
NCIE-2
NCIE-1
δ13CTOC
Sample/depth (m)
Coastal SEG
Riverine SEG
Wet lowland SEG
Dry lowland SEG
Hinterland SEG
PC 1
PC 2
Hygrophyte/xerophyte ratio
Kaolinite%
Kaolinite/illite ratio
from Dal Corso et al. (2018)
[Percentages%]
-humidiy+
-proximity+
Veszprém-1 section
Csicsó Marl
SDM
First local appearance of Aulisporites astigmosus
First local appearance of Lagenella martinii

Figure 8

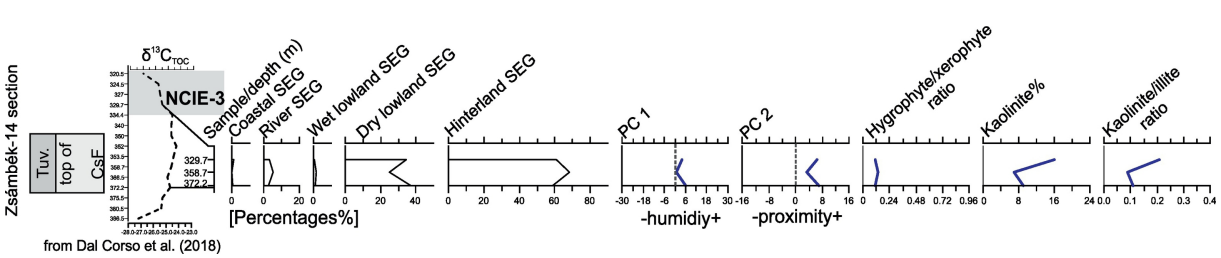
Zsámbék-14 section
Tuv.
top of
CsF
δ13CTOC
NCIE-3
329.7
358.7
372.2
from Dal Corso et al. (2018)
Sample/depth (m)
Coastal SEG
River SEG
Wet lowland SEG
Dry lowland SEG
Hinterland SEG
[Percentages%]
PC 1
-humidiy+
PC 2
-proximity+
Hygrophyte/xerophyte ratio
Kaolinite%
Kaolinite/illite ratio

Figure 9

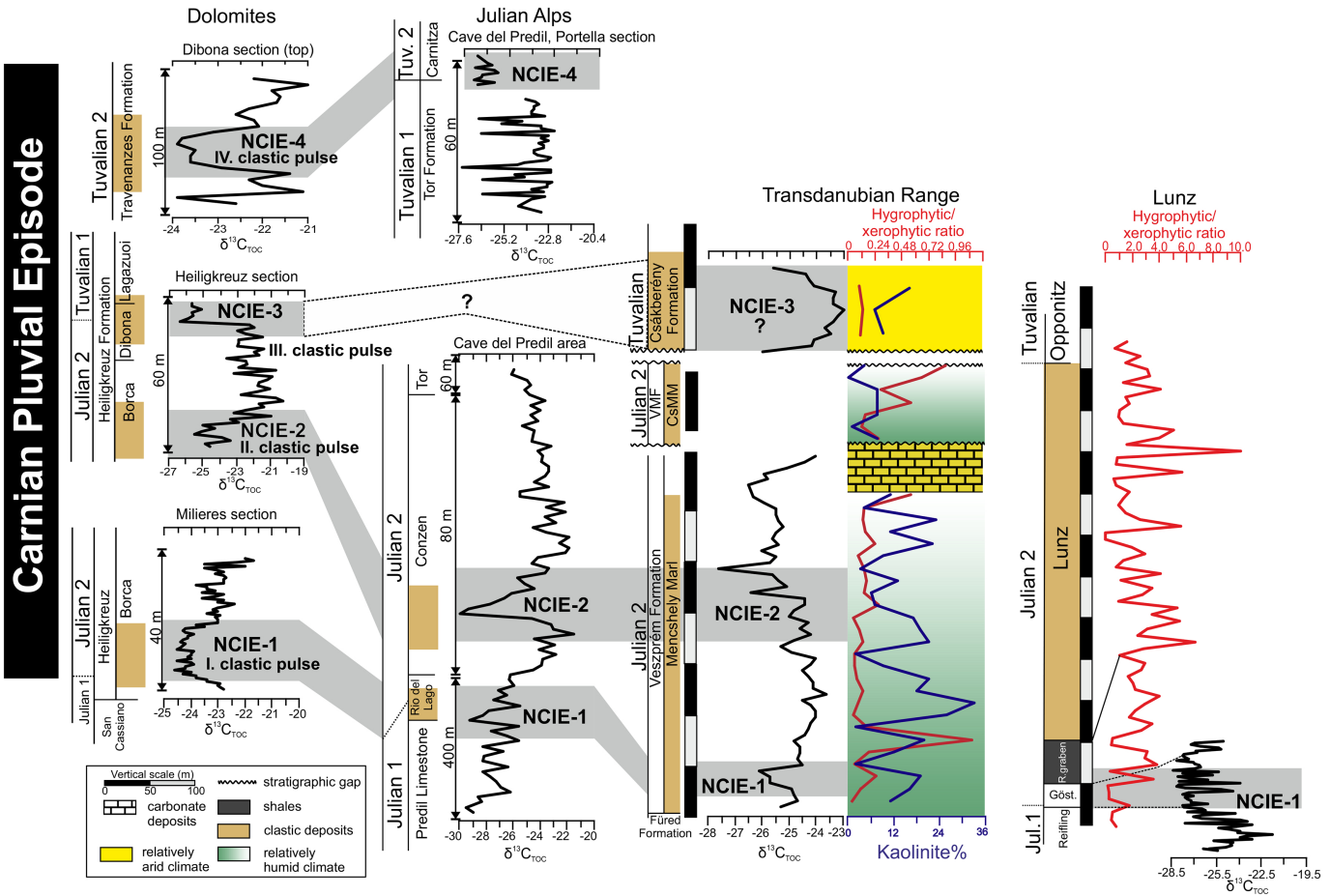
Carnian Pluvial Episode
Dolomites
Dibona section (top)
Tuvalian 2
Travenanzes Formation
NCIE-4
IV. clastic pulse
100 m
Julian Alps
Cave del Predil, Portella section
Tuv. 2
Carnitza
Tuvalian 1
Tor Formation
NCIE-4
60 m
Heiligkreuz section
Tuvalian 1
Julian 2
Heiligkreuz Formation
Dibona
Lagazuoi
Borca
NCIE-3
III. clastic pulse
NCIE-2
II. clastic pulse
60 m
Milieres section
Julian 2
Heiligkreuz
Borca
Julian 1
San Cassiano
NCIE-1
I. clastic pulse
40 m
Cave del Predil area
Julian 2
Conzen
Tor
Rio del Lago
80 m
60 m
400 m
NCIE-2
NCIE-1
Julian 1
Predil Limestone
Transdanubian Range
Hygrophytic/ xerophytic ratio
Tuvalian
Csákberény Formation
NCIE-3
?
Julian 2
VMF
CsMM
Veszprém Formation
Mencshely Marl
NCIE-2
NCIE-1
Füred Formation
Kaolinite%
Lunz
Hygrophytic/ xerophytic ratio
Tuvalian
Opponitz
Julian 2
Lunz
R.graben
Göst.
Jul.1
Reifling
NCIE-1
Vertical scale (m)
carbonate deposits
relatively arid climate
stratigraphic gap
shales
clastic deposits
relatively humid climate
δ13CTOC

Figure 10